HIF-1 is a protective factor in conditional PHD2 deficient mice suffering from severe HIF-2 -induced excessive erythropoiesis

Franke, Kristin ; Kalucka, Joanna ; Mamlouk, Soulafa ; Singh, Rashim Pal ; Muschter, Antje ; Weidemann, Alexander ; Iyengar, Vasuprada ; Jahn, Steffen ; Wieczorek, Kathrin ; Geiger, Kathrin ; Muders, Michael ; Sykes, Alex M ; Poitz, David ; Ripich, Tatsiana ; Otto, Teresa ; Bergmann, Sybille ; Breier, Georg ; Baretton, Gustavo ; Fong, Guo-Hua ; Greaves, David R ; Bornstein, Stefan ; Chavakis, Triantafyllos ; Fandrey, Joachim ; Gassmann, Max ; Wielockx, Ben

Abstract: Erythropoiesis must be tightly balanced in order to guarantee adequate oxygen delivery to all tissues in the body. This process relies predominantly on the hormone erythropoietin (EPO) and its transcription factor hypoxia inducible factor (HIF). Accumulating evidence suggests that oxygen-sensitive prolyl hydroxylases (PHDs) are important regulators of this entire system. Here, we describe a novel mouse line with conditional PHD2 inactivation (cKO P2) in renal EPO producing cells, neurons and astrocytes that displayed excessive erythrocytosis due to severe over-production of EPO, exclusively driven by HIF-2 . In contrast, HIF-1 served as a protective factor, ensuring survival of cKO P2 mice with hematocrit values up to 86%. Using different genetic approaches, we show that simultaneous inactivation of PHD2 and HIF-1 resulted in a drastic PHD3 reduction with consequent overexpression of HIF-2 -related genes, neurodegeneration and lethality. Taken together, our results demonstrate for the first time that conditional loss of PHD2 in mice leads to HIF-2 -dependent erythrocytosis, whereas HIF-1 protects these mice, providing a platform for developing new treatments of EPO-related disorders like anemia.

DOI: https://doi.org/10.1182/blood-2012-08-449181

HIF-1α is a Protective Factor in Conditional PHD2 Deficient Mice Suffering from Severe HIF-2α-Induced Excessive Erythropoiesis

Kristin Franke[1,2], Joanna Kalucka[1,2], Soulafa Mamlouk[1,2], Rashim Pal Singh[1,2], Antje Muschter[1,2], Alexander Weidemann[3], Vasuprada Iyengar[1,2], Steffen Jahn[2], Kathrin Wieczorek[2], Kathrin Geiger[2], Michael Muders[2], Alex M. Sykes[4], David Poitz[5], Tatsiana Ripich[6], Teresa Otto[7], Sybille Bergmann[8], Georg Breier[2,9], Gustavo Baretton[2], Guo-Hua Fong[10], David R. Greaves[11], Stefan Bornstein[12], Triantafyllos Chavakis[12], Joachim Fandrey[7], Max Gassmann[13] and Ben Wielockx[1,2,9]

[1]Emmy Noether Research Group. [2]Institute of Pathology, University of Technology, Dresden, Germany. [3]Department of Nephrology and Hypertension, University Clinic Erlangen, Germany. [4]Max Planck Institute of Molecular Cell Biology and Genetics, Dresden, Germany. [5]Department of Internal Medicine and Cardiology, University of Technology, Dresden, Germany. [6]Institute of Physiological Chemistry, University of Technology, Dresden, Germany. [7]Department of Physiology, University of Duisburg-Essen, Essen, Germany. [8]Institute of Clinical Chemistry and Laboratory Medicine, University of Technology, Dresden, Germany. [9]DFG Research Center and Cluster of Excellence for Regenerative Therapies Dresden, University of Technology, Dresden, Germany. [10]Center for Vascular Biology, Department of Cell Biology, University of Connecticut Health Center, Farmington, CT. [11]Sir William Dunn School of Pathology, University of Oxford, UK. [12]Department of Medicine III, Carl Gustav Carus University Hospital, Dresden, Germany. [13]Institute of Veterinary Physiology, Vetsuisse Faculty and Zurich Center for Integrative Human Physiology (ZIHP), University of Zürich, Switzerland and Universidad Peruana Cayetano Heredia (UPCH), Lima, Peru.

Authors notes: Kristin Franke, Joanna Kalucka, Soulafa Mamlouk and Rashim Pal Singh contributed equally to this work. Present address of Joanna Kalucka: Department of Nephrology and Hypertension, University Clinic Erlangen, Germany.

Address correspondence to: Ben Wielockx, Emmy Noether group (DFG) Inst. of Pathology - University of Technology Dresden, Schubertstrasse 15, D-01307 Dresden, Germany; Tel: +49-351 4585257; Fax: +49-351 4584328; Ben.Wielockx@uniklinikum-dresden.de

Abstract

Erythropoiesis must be tightly balanced in order to guarantee adequate oxygen delivery to all tissues in the body. This process relies predominantly on the hormone erythropoietin (EPO) and its transcription factor hypoxia inducible factor (HIF). Accumulating evidence suggests that oxygen-sensitive prolyl hydroxylases (PHDs) are important regulators of this entire system. Here, we describe a novel mouse line with conditional PHD2 inactivation (cKO P2) in renal EPO producing cells, neurons and astrocytes that displayed excessive erythrocytosis due to severe over-production of EPO, exclusively driven by HIF-2α. In contrast, HIF-1α served as a protective factor, ensuring survival of cKO P2 mice with hematocrit values up to 86%. Using different genetic approaches, we show that simultaneous inactivation of PHD2 and HIF-1α resulted in a drastic PHD3 reduction with consequent overexpression of HIF-2α-related genes, neurodegeneration and lethality. Taken together, our results demonstrate for the first time that conditional loss of PHD2 in mice leads to HIF-2α-dependent erythrocytosis, whereas HIF-1α protects these mice, providing a platform for developing new treatments of EPO-related disorders like anemia.

Introduction

Erythropoietin (EPO) is the primary regulator of red blood cell formation and its expression level is extremely responsive to fluctuations in tissue oxygenation. Dysregulation of EPO production can lead to either anemia, if levels are inadequately low, such as in terminal kidney failure or to erythrocytosis if levels are inappropriately high. Erythrocytosis will develop when EPO is continuously overproduced, causing the generation of new erythrocytes at a rate exceeding the removal of senescent red blood cells.[1] In adult animals the main physiological source of EPO is the kidney, although the liver as well as the central nervous system (CNS) have also been shown to produce EPO but to a much lesser extent.[2,3] The main physiological stimulus of EPO production is tissue hypoxia in the interstitium of the kidney.[4] Already two decades ago it was shown that this effect was dependent on binding of the transcription factor hypoxia inducible factor (HIF) to 5'- and 3′-enhancer regions of the *EPO* gene, known as the hypoxia responsive element (HRE).[5]

HIF is a heterodimeric complex composed of an oxygen-sensitive HIFα and a constitutive HIFβ subunit. Of the most intensively studied HIF-α genes, HIF-1α has a ubiquitous pattern of expression in all tissues,[6] whereas expression of the paralogue HIF-2α is restricted to certain cell types.[7,8] However, both factors actively promote oxygen delivery and adaptive processes to hypoxia such as erythropoiesis, angiogenesis, anaerobic glycolysis and hematopoiesis.[1,9-11] Oxygen-sensing is therefore indispensable as it enables the cells to instantaneously adapt to an inappropriately low pO_2. This machinery relies on the HIF-prolyl hydroxylases (PHD1-3), enzymes that hydroxylate and, consequently, lead to the inactivation of HIFα in the presence of oxygen.

PHD2 is believed to be the crucial oxygen sensor during normoxia and mild hypoxia,[12] which is underscored by the fact that inactivation of PHD2 severely deregulates normal embryonic development resulting in embryonic lethality by E14.5, whereas PHD1-/- or PHD3-/- mice develop normally.[13] Moreover, even haplodeficient PHD2+/- mice show normalization of the endothelial lining during tumor development compared to wild type controls.[14] In humans, several heterozygous point mutations in the *PHD2* gene have been described, which lead to an absolute increase in red blood cell mass. These are in some cases associated with severe clinical conditions like hemorrhage, stroke and increased risk of thrombosis,[15-18] although the latter was shown to be independent of elevated hemoglobin/hematocrit.[19] PHD2 is therefore the main HIF prolyl hydroxylase isoform which, next to HIF-2α and the von Hippel-Lindau protein (VHL), controls the expression of EPO in humans[20]. In spite of the above, the role of PHD2 in the etiology of erythrocytosis and related disorders has not been extensively studied. Indeed, systemic PHD2 heterozygosity in mice shows only a very mild induction of hematocrits[14], whereas somatic inactivation shortly before or after birth leads to severe erythrocytosis and early lethality.[21,22]

In this report, we describe a new conditional PHD2 mouse line expressing cre-recombinase under the control of the modified human CD68 promoter, commonly defined as a monocyte/macrophage marker.[23] In addition, we found PHD2-loss in other cell lineages, resulting in excessive HIF-2α-induced EPO production in kidney and brain, extreme hematocrits up to 86%, thrombocytopenia and splenomegaly, but survival of the mice in a HIF-1α-dependent manner. Additional inactivation of HIF-1α (PHD2/HIF-1α double knockout) leads to early lethality around adulthood, which is confined to PHD3-reliant HIF-2α-overstabilization and consequent neurodegeneration in the brain.

Taken together, our results establish a principal role for PHD2 as an oxygen sensor in CD68-positive cells for the HIF-2α-dependent regulation of EPO and highlight a protective role of HIF-1α in polycythemic mice.

Methods

Generation of a CD68:cre line

The modified hCD68-IVS1 promoter,[23] which combines the 2940 bp of sequence 5' to the ATG and the 83-bp first intron of the human CD68 gene was cloned just in front a codon-improved *Cre* recombinase sequence (1091 bp)[24] and a polyA signal. Different founders were produced and tested on expression levels in isolated peritoneal F4/80$^+$ cells. Finally, two lines were selected of which one expressed cre-recombinase already in sperm as well as egg cells. The other transgenic line was intercrossed with PHD2$^{f/f}$ mice and used in the current report.

Mice

All mice were housed at the Experimental Centre at the University of Technology Dresden (Medical Faculty, University Hospital Carl-Gustav Carus), under specific pathogen-free conditions. Experiments were performed with male and female mice at the age of 8-12 weeks or as stated in the text. All mice described in this report were born in a normal Mendelian manner. HIF-2α $^{f/f}$ mice were obtained from The Jackson Laboratories (Bar Harbor, Maine) and originally produced in the research group of Dr. C. Simon[25]. All mouse strains were at least nine generations backcrossed to C57BL/6. Mice were genotyped using primers described in Table S1. The construction and identification of the PHD2$^{f/f}$ mouse line will be described elsewhere (R.P.S, K.F., J.K., S.M., A.M., B.W. unpublished results).

More than 60% of all CD68:cre-PHD2$^{f/f}$ (cKO P2), CD68:cre-PHD2/HIF-1α$^{ff/ff}$ (cKO P2/H1) and CD68:cre-PHD2/PHD3$^{ff/ff}$ (cKO P2/P3) mice showed redness of snout/paws associated with high hcts (> ~70%) and were used for the described experiments. Non-erythrocytotic cKO, cKO P2/H1 and P2/P3 mice all showed hematocrits comparable to WT littermates (<55%), which was always related with lower penetrance of cre-recombinase activity and were only used for breeding. No cKO mice were found with hematocrits between 55 and 70%. Penetrance in cKO P2/H1, CD68:cre-PHD2/HIF-2α$^{ff/ff}$ (cKO P2/H2), CD68:cre-PHD2/PHD3$^{ff/ff}$ (cKO P2/P3), CD68:cre-HIF-1α$^{f/f}$ (cKO H1) and CD68:cre-HIF-2α$^{f/f}$ (cKO H2) mice was defined via qRT-PCR on BM mRNA and/or genomic PCR on ear biopsies. Knock-down efficiencies for HIF-1α and HIF-2α in these genotypes were comparable to expression levels for PHD2. It is noteworthy that only a low percentage (~20%) of cKO P2/H2 mice showed cre activity with high penetrance on both alleles simultaneously. Only these mice were considered for the presented experiment. All other mice, carrying CD68:cre-PHD2$^{f/f}$ and HIF-2α$^{f/f}$, showed no targeting or only of one of the alleles. All animal experiments were in accordance with the facility guidelines on animal welfare and were approved by the Landesdirektion Dresden, Germany.

Blood analysis

Blood parameters (hematocrit, RBCs, Hb and thrombocytes) were measured using a Sysmex automated blood cell counter (Sysmex XE-2100 and XE-5000). Plasma erythropoietin and thrombopoietin concentrations were determined using the Quantikine Mouse/Rat EPO immunoassay and the Quantikine Mouse Tpo immunoassay (R&D Systems).

Blood pressure and heart rate were measured non-invasively with the tail cuff method (UGO BASILE). After training of the animals for two weeks, the average of at least two independent measurements was calculated.

Cells

The human kidney cell line REPC was cultivated as described previously.[26] *Astrocytes* were isolated from the cerebral cortex of five day old pups by incubation with 0.025% Trypsin for 30 minutes, followed by enrichment with the biotinylated anti-GLAST (ACSA-1) antibody (Miltenyi Biotec) and magnetic beads. The highly enriched astrocyte fraction (purity >90%) was confirmed via FACS (data not shown).

Isolation of individual cell types

Primary mouse keratinocytes and fibroblasts were isolated from newborn mice by incubating the skin with 250mg/ml Dispase (Roche) overnight at 4°C. The epidermal layer was separated from the dermal layer and incubated in TrypLE select enzyme (Invitrogen) for 30 min at RT. The resulting single cell suspension was cultured in CnT medium (Cell-n-Tech). The dermal layer was finely minced and then incubated in a 0.25% trypsin / EDTA solution (Gibco) for 30 min at 37°C. The resulting cell suspension was cultured in DMEM (Lonza) containing 10% FBS (Biochrom), 1% L-Glutamine (Lonza) and 1% penicillin/streptomycin (Lonza). Identity of keratinocytes was confirmed via Keratin6 (K6) staining (data not shown). Enterocytes were isolated from 2 cm of colon starting from the caecum. The colon was cut into 5-6 pieces and incubated in Cell Recovery Solution (BD Biosciences) for 1.5 h at 4°C. After vigorous shaking, the cell suspension was filtered, centrifuged, and the resulting cell pellet frozen. Identity of the

enterocytes (colonocytes) was confirmed via Villin1 staining (data not shown). Endothelial cells were isolated from the lung via FACS ($CD31^+CD34^+$) and confirmed on the basis of CD31 mRNA expression (data not shown).

Expression analysis

RNA from organs and sorted cells was isolated using RNeasy Mini Kit (Qiagen), NucleoSpin RNA XS (Machery-Nagel), Trizol (Invitrogen), Universal RNA Purification Kit (roboklon) or DNA+RNA+PROTEIN Purification Kit (roboklon). cDNA was synthesized using random primers (Roche) and SuperScript II (Invitrogen). Expression levels were determined by performing quantitative Real-time PCR using the Maxima SYBR Green QPCR Master Mix (Fermentas) on an iCycler iQ (Biorad). Sequences of primers used are given in Table S2. Expression levels were normalized with the ΔΔCt method using primers given in Table S3.

Histology and immunofluorescence

For all samples, organs were placed in 4% formaldehyde at 4°C overnight, dehydrated, embedded in paraffin and cut. Sections were rehydrated and subjected to hematoxylin and eosin staining or acidic Fuchsin orange G-staining. For IHC, antigen retrieval (citrate buffer-PH 6.0) at 95°C for 20 minutes was performed on rehydrated sections. Incubation with primary antibody (Ab) ((Iba1 (WAKO), cleaved-Caspase3 (Cell Signaling), NeuN (Abcam)) was 1.5h at 37°C. Secondary Ab were Alexa-488 or Alexa-568 (Molecular Probes) incubated for 30 min. at RT. Cell nuclei were stained with DAPI. Slides were mounted with fluorescent mounting media (Dako). For frozen sections, samples were embedded in OCT, cut and stored at -20°C. For immunofluorescence staining, sections were first fixed for 10 min in cold acetone and blocked

with 5% goat serum in TNT buffer (20mM Tris pH 7.6, 0.9% NaCl, 0.05% Tween in PBS). Thereafter, sections were incubated with mouse anti-NeuN and rabbit anti-PHD2 at 37°C for 1h (custom-made polyclonal rabbit anti-mouse antibody against a C-terminal peptide of PHD2 (EKGVRVELKPNSVSKDV) and purified via a peptide sulfoLink immobilization column (Pierce, ThermoScientific, IL)). Secondary antibody as described above.

Microscopy

Fluorescent and light microscopy was done with an Axioplan-2 imaging microscope and plan Apochromat lenses (Carl Zeiss). The cameras and acquisition software were either Q Imaging Retiga 2000R and Image pro MC6.0 (fluo) or Axiocam MRc5 and Axiovision (light). Image processing and analysis was done using ImageJ and the ImageJ distribution Fiji (http://pacific.mpi-cbg.de/wiki/index.php/Fiji).

Flow cytometry

FACS analysis was performed on LSRII (Becton Dickinson), sorting was done on Aria II (Becton Dickinson). Cell numbers were counted on MACS quant (Miltenyi). Data was analyzed on DIVA (Becton Dickinson), MACS quantify (Miltenyi) or Flowjo (Treestar) software. BM single cell suspensions were made by flushing the marrow using 23G needles. Single cell suspensions from spleen and lymph nodes were prepared by manual disruption using frosted slide ends, additionally for spleen cells enzymatic digestion was performed with 0.3U/ml Collagenase D (Roche) for 40 min at 37°C. The lineage cocktail included CD3 (145-2C11, eBioscience), CD19 (eBio1D3, eBioscience), NK1.1 (PK136, eBioscience), Ter119 (Terr119, eBioscience), CD11b (M1/70, eBioscience), Gr1 (RB6-8C5, eBioscience), B220 (RA3-6B2,

eBioscience), CD127 (A7R34, eBioscience), CD11c (N418, eBioscience). For MEP analysis, spleen and bone marrow cells along with lineage cocktail were also incubated with c-kit (APC, 2B8, eBioscience), Sca1 (Pe-Cy7, D7, eBioscience), CD16/32 (A700, 93, eBioscience), CD34 (FITC, RAM34, eBioscience), SA (PerCP, BD Biosciences). 1 x10^6 cells from bone marrow and 2 x10^6 cells from spleen were acquired. For EB analysis, spleen and bone marrow cells were stained with CD71 (FITC, R17217, eBioscience) and Ter119 (Pe-Cy7, Ter119, eBioscience). 2 x 10^5 cells were acquired. For lymphoid cell analysis, spleen and lymph node cells were incubated with CD3 (APC, 145-2c11, eBioscience) and CD19 (FITC, MB19-1, eBioscience). For myeloid cell analysis, spleen cells were incubated with CD11b (PE, M1/70, eBioscience), F4/80 (PerCP-cy5.5, BM8, eBioscience) and/or Gr1 (A700, RB6-8C5, eBioscience).

Blood volume determination

Blood was collected in EDTA vials, washed twice with 0.9% NaCl, and stained with 15uM Vybrant DiI Cell-labeling solutions (Invitrogen) for 2.5h at RT on a tilt shaker. After washing and re-suspension in PBS 100ul was injected intravenously. One hour later a blood sample was taken from the mouse, diluted and analyzed for DiI containing cells.

Statistical analysis

Data and graphs represent mean ± SEM of representative experiments. Statistical significance was calculated as two-tailed by the Mann Whitney U test (GraphPad Prism v5.04), with $p<0.05$ considered statistically significant.

Results

Conditional PHD2 deficient mice display severe HIF-2α-dependent erythrocytosis

PHD2 is the main HIF prolyl hydroxylase isoform, which controls the expression of EPO in humans.[20] Somatic inactivation of PHD2 shortly before or after birth leads to severe polycythemia probably in a HIF-1α-dependent manner but is accompanied by early lethality and has therefore not been extensively studied.[21,22] To conditionally ablate PHD2, we first generated a $PHD2^{f/f}$ mouse line by gene targeting using a construct in which Exons 2 and 3 are flanked by loxP sites (R.P.S, K.F., J.K., S.M., A.M., B.W. unpublished results). We combined this with a newly designed mouse line expressing cre-recombinase under the control of the modified human CD68 promoter, known as a monocyte/macrophage marker (Supplemental Figure 1A). Thorough analyses revealed that these cKO P2 mice are not only significantly deficient for PHD2 in macrophages, but in the entire hematopoietic system (bone marrow) (Supplemental Figure 1B). In addition, we also found a profound PHD2 reduction in a few subsets of epithelial cells (e.g. keratinocytes and colonocytes), but not in other cell lineages like endothelial cells (ECs) and fibroblasts (Supplemental Figure 1C). In the lysates of non-hematopoietic organs studied in the current report, we found no significant reduction of PHD2 expression (Supplemental Figure 1D). Moreover, no significant compensation by one of the other PHDs could be shown (Supplemental Figure 1E)

Interestingly, the majority of these cKO P2 mice showed obvious redness of paws and snout starting around 4 weeks of age, which was accompanied by significant growth retardation until adulthood (Figure 1A-B). This striking phenotype was due to elevated hematocrits which increased with age to >85% in some individuals (Figure 1C). However, although the blood viscosity was substantially increased, we observed no difference in the blood pressure, heart rate

or cardiac hypertrophy, as has been shown before for other erythrocytotic mice (Supplemental Figure 2A-B).[27] As PHD2 can control the activity of both HIF-1α and HIF-2α we determined which of the HIFs contributed to the erythrocytosis. The notion that HIF-2α acts as the main regulator of EPO is based on histological and genetic approaches in HIF-2α deficient mice.[10,25,28] Moreover, several studies in patients with idiopathic erythrocytosis revealed the presence of different heterozygous missense mutation in the coding sequence of HIF-2α, but not HIF-1α, leading to impaired PHD2-induced hydroxylation.[29,30] On the other hand, a somatic knockout of PHD2, suggested that HIF-1α, rather than HIF-2α, contributed to increased renal EPO synthesis.[21] To unequivocally determine the major regulator in the erythrocytotic cKOs, we therefore generated mice double deficient for PHD2 and HIF-1α or HIF-2α. Our data demonstrate that the erythrocytosis phenotype as shown in cKO P2 mice was abolished in CD68:cre-PHD2/HIF-2α$^{ff/ff}$ mice (cKO P2/H2), displaying even significantly lower hematocrits and hemoglobin levels than in WT mice (Figure 1D-F). On the other hand, hematocrits in CD68:cre-PHD2/HIF-1α$^{ff/ff}$ mice (cKO P2/H1) were indistinguishable from cKO P2, showing that PHD2-induced severe erythrocytosis is exclusively dependent on HIF-2α but not on HIF-1α. These results are emphasized by the fact that conditional knock-down of HIF-2α alone (CD68:cre-HIF-2α$^{f/f}$ (cKO H2)), but not HIF-1α (CD68:cre-HIF-1α$^{f/f}$ (cKO H1)), already resulted in a mild anemia (Supplemental Figure 3A-C).

Erythrocytosis is EPO dependent and associated with increased EPO expression in kidney and brain

Since excessive secondary erythropoiesis is mainly mediated by erythropoietin (EPO),[27] we measured EPO plasma levels in both erythrocytotic mouse lines (cKO P2 and cKO P2/H1) and

found a highly significant induction of EPO expression in cKO P2 mice compared to WT littermates. Surprisingly, although cKO P2/H1 mice showed similar hematocrits to cKO P2 mice, they contained on average 2.5-fold higher plasma EPO values than cKO P2 mice (Figure 2A). The main source of EPO in adult mice is the kidney,[3] where we found a 10-fold and 20-fold increase of EPO in extracts from cKO P2 and from cKO P2/H1 mice, respectively. Additionally, the expression of EPO in the brain was significantly up-regulated (Figure 2B). In contrast, hepatic EPO expression levels were very low, and no increase could be observed in any of the mice (data not shown).

In the kidney, EPO is produced by specialized interstitial cells localized in the deep cortex between the proximal tubular and vascular endothelial cells. These renal EPO producing (REP) cells also express neuronal-specific markers but isolation of these primary cells has been a real challenge so far.[31] Therefore, we tested the recently described human REP cell line, isolated from the tumor-free tissue of a male patient[26] and demonstrate that these cells co-expressed both CD68 and EPO, supporting the link between CD68-driven cre expression, PHD2 inactivation and subsequent EPO expression in our cKO P2 mice (Figure 2C). In the brain, astrocytes and neurons are known to be sources of EPO.[32] We therefore isolated astrocytes from the cerebral cortex of five day old pups and found a significant PHD2 reduction in cKO P2 cells versus WT (Figure 2D). The latter result was similar to the knockdown efficiency found in other cell types (Supplemental Figure 1B-C). Via IHC we demonstrate that sections from adult cKO P2 brains contain a majority of PHD2-negative cells that were positive for the neuronal marker NeuN (Figure 2E).

Moreover, since cKO P2 mice are also deficient for PHD2 in the BM, we transplanted BM cells from cKO P2 mice into lethally irradiated WT mice and vice-versa. However, we found no

significant difference in hematocrit compared to non-transplanted animals, thus excluding the possibility that the phenotype could be transferred with PHD2-deficient hematopoietic cells (Figure 2F).

Taken together, the erythrocytosis phenotype in cKO P2 and cKO P2/H1 mice is correlated with an enormous induction of EPO in the kidney and the brain, related to PHD2 inhibition in REP cells, astrocytes and neurons.

Erythrocytosis is mainly caused by extramedullary erythropoiesis. Basal erythropoiesis mainly takes place in the bone marrow whilst the spleen can increase its capability to produce RBCs under conditions of stress erythopoiesis.[33] In the cKO P2, polycythemia resulted in splenomegaly accompanied by loss of splenic architecture, with an increase in nucleated cells and total weight (Figure 3A-C). Remarkably, the megakaryocyte-erythroid progenitors (MEPs) were found to be significantly induced (>2.5 fold) in the spleen of cKO P2 mice but not in BM (Figure 3D-E). In addition, splenic $CD71^+/Ter119^+$ erythroblasts (EBs) were increased more than 10-fold in cKO P2 mice compared to WT littermates, whereas only a mild increase in EBs was found in BM (Figure 3F-G). The fraction of B- and T-cells were markedly decreased in the cKO P2 spleen while lymph nodes contained an excess of both populations, suggesting that there is no impairment of their production but only a difference in localization due to the EB excess in the spleen (Supplemental Figure 4A-D). Splenic $CD11b^+F4/80^+$ macrophages and neutrophils (PMNs) were not significantly altered, although red pulp macrophages, a distinct subset of macrophages involved in the removal of senescent erythrocytes, were highly induced in the cKO P2 spleen (Supplemental Figure 4E-G). These results imply that the spleen is primarily responsible for the overproduction of RBCs in cKO P2 mice.

Thrombocytopenia is directly related to the higher blood volume

Further hematological analysis revealed a significant decrease in platelet numbers in cKO P2 mice compared to WT mice, as early as at 4 weeks of age (Figure 4A). This effect was also related to HIF-2α but not HIF-1α, since the phenotype was rescued only in the cKO P2/H2 mice (Figure 4B). To examine the molecular background of this effect we analyzed different parameters but found no relative difference in thrombopoietin (TPO), the number of megakaryocytes in the BM or spleen (Supplemental Figure 5A-C), nor did we detect micro-vascular thrombosis, which would have indicated increased consumption of platelets (Figure 4C-D). However, using flow cytometry on labeled RBCs, we found that the total blood volume in cKO P2 mice was significantly increased by about 65% (Figure 4E); strongly suggesting that the reduced platelet count is a dilution effect.

cKO P2 mice display a normal life span whilst cKO P2/H1 die early. One common feature of the somatic PHD2 deficient mice[21,22] as well as other EPO-related erythrocytotic mice[34,35] is that these mice die prematurely. Surprisingly, we never observed any premature death in our cKO P2 mice. Moreover, we did not encounter any lethality in a group of nine erythrocytotic cKO P2 mice that were maintained for over twenty months. These mice were bled every four months but no significant drop in hematocrit could be observed (Figure 4F). Finally, all mice were sacrificed and several organs examined in great detail. Except for a regressing cyst associated with the ovary of one mouse (Supplemental Figure 6A), no obvious pathological defects or tumors were detected (Supplemental Figure 6B). On the other hand, the cKO P2/H1 mice started to die very sudden from week five onwards, and by week sixteen 95% of these mice were dead (mean

survival time: 11 weeks) (Figure 4G). In contrast, neither cKO P2/H2 nor cKO H1 or H2 mice showed any premature death. Importantly, these results show for the first time that extremely high hematocrits do not necessarily lead to lethality or pathological abnormalities in part due to a protective function of HIF-1α.

Simultaneous loss of PHD2 and HIF-1α in the brain leads to neurodegeneration

In order to investigate the biological background of the early lethality of cKO P2/H1 mice, we conducted a thorough examination of 8-10 week old living as well as recently-deceased cKO P2/H1 mice. No acute cardiovascular complications or obvious evidence for thrombosis or degeneration in different examined organs were observed (data not shown). However, via IHC staining we detected a dramatic induction of activated ($Iba1^+$) microglia cells in the brain of cKO P2/H1 mice compared to WT and cKO P2 mice (Figure 5A-C). This strongly suggests that pathological changes in cKO P2/H1 brains led to the activation of these resident macrophages. Consistent with this, we found numerous patches of neurons ($NeuN^+$) in cKO P2/H1 brain sections, especially from freshly deceased mice, that showed strong expression of cytoplasmic cleaved-caspase3 (Cl-Casp3), indicative of apoptosis (Figure 5D-F). In contrast, no Cl-Casp3 staining could be detected in cKO P2 or WT brains (data not shown). In line with the observed phenotype, we found that some (3 out of 16) of the cKO P2/H1 mice even displayed a dome-shaped skull accompanied by a dramatic hydrocephalus (Supplemental Figure 7A-B).

To unravel the molecular background of this neurodegeneration, we compared the gene profiles of cKO and cKO P2/H1 brains. Remarkably, *PHD3*, a HIF-1α -regulated gene and formerly identified as a very potent negative regulator of HIF-2α,[36] was drastically down-regulated in cKO P2/H1 brains compared to cKO P2 counterparts. Conversely, we found a significant

induction of pro-inflammatory cytokines like *TNFα, Il-1α* and *IL-1β*, as well as *VEGFA*, *TGFβ1*, *CXCR4* and *adrenomedullin* (*Adm*) (Figure 5G), many of which have been shown to be HIF-2α-dependent genes.[37] These data therefore suggest that knocking out *HIF-1α* in addition to PHD2 in a subset of brain cells (e.g. astrocytes and microglia cells) leads to an additional stabilization of HIF-2α and consequent transcriptional activation of a variety of genes, including detrimental inflammatory cytokines that can contribute to neurodegeneration and lethality of the cKO P2/H1 mice.

To evaluate whether HIF-1α-induced *PHD3*-expression is directly related to the protection of cKO P2 mice, we developed mice lacking PHD2 and PHD3[13] in $CD68^{+}$ cells (CD68:cre-$PHD2/PHD3^{ff/ff}$ (cKO P2/P3)). Interestingly, these mice did not only display severe erythrocytosis (Figure 6A); a majority of them suddenly died starting shortly after birth (Figure 6B), whereas cKO P2 as well as $PHD3^{-/-}$ mice never died during this period. Furthermore, we isolated the brains of these cKO P2/P3 mice and analyzed the same array of genes as we studied for the cKO P2/H1 animals. Interestingly, we found that virtually all differentially expressed genes in brain lysates from cKO P2/H1 mice are also significantly changed in the brains of cKO P2/P3 mice, compared to cKO P2 (Figure 6C). These data strengthen our hypothesis that PHD3 is a not only a protective factor in the brain of cKO P2 mice, but acts downstream of HIF1α. Taken together, these results reveal a tight and essential balance between HIF-1α and HIF-2α activity in the brain, which also involves the PHD3 regulation.

Discussion

In the current study we used a genetic approach to investigate in detail the biological role of PHD2 in CD68-positive cells and the relation of two of its substrates (HIF-1α and HIF-2α) with

erythropoietin production and during erythropoiesis. We have demonstrated that conditional PHD2 deficient mice are able to cope with extreme numbers of RBCs, thrombocytopenia and splenomegaly through a discrete interplay between HIF-1α and HIF-2α involving the regulation of PHD3.

Although CD68 has been described as a marker mainly limited to monocytic cells,[23] our data demonstrate at least temporary expression in the hematopoietic compartment as well as in subsets of epithelial lineages, but not in ECs or fibroblasts. Moreover, our results demonstrate loss of PHD2 in a subset of renal and brain cells responsible for the production of EPO, which leads to massive stress erythropoiesis primarily executed by the adult spleen. Remarkably and in clear contrast to many other reports,[3,21,22,35] our erythrocytotic cKO P2 mice show normal lifespan, demonstrating that an unusual high hematocrit is not per se lethal; a phenomenon that has also been described in a few healthy cobalt miners at high altitude that developed hematocrits ranging from 75-91%.[38] Genetically, a number of heterozygous *PHD2* missense mutations have been defined in patients, which impair the binding to both HIF-1α and HIF-2α resulting in erythrocytosis.[15-18] One patient with such a *PHD2* mutation and consequent polycythemia developed a paraganglioma, suggesting that PHD2 may act as a tumor suppressor.[1] However, our results strongly suggest that sustained exposure to high levels of EPO and permanent loss of *PHD2* in different cell types does not necessarily lead to spontaneous tumor development over a period of 20 months in mice. This has also been underscored by recent work from our group showing that silencing of PHD2 in several tumor lines typically leads to reduced tumor growth.[39]

In mice, we (K.F. and B.W., unpublished data) and others[14] have shown that *PHD2* heterozygosity only results in a very mild form of erythrocytosis whereas global inactivation just

before or after birth leads to severe and lethal polycythemia.[21,22] Based on expression levels in the kidney of the latter mice, it was proposed that HIF-1α, rather than HIF-2α, might be the central erythrocytosis mediator in relation to PHD2.[21] However, our genetic approach (PHD2/HIFα double deficient mice) clearly shows that this phenotype is driven by HIF-2α. The notion that only HIF-2α induces EPO is not new,[25,28] and is in line with observations from Percy and colleagues in familial erythrocytosis.[29,30] However, to the best of our knowledge this is the first report that shows that PHD2-induced severe erythrocytosis is exclusively dependent on HIF2α and not on HIF1α. In addition, the finding that CD68:cre-HIF-2α$^{f/f}$ mice were mildly anemic emphasizes the importance of this HIF-subunit and confirms the, at least temporary, activity of CD68, in specialized EPO-producing cells.

Simultaneous ablation of PHD2 and HIF-1α on the other hand led to early lethality, clearly demonstrating that HIF-1α acts as a crucial survival factor in the erythrocytotic cKO P2 mice. In particular, detailed analysis of mature cKO P2/H1 mice showed pathological defects only in the brain, a feature that was underlined by the severe hydrocephalus we observed in a few of the cKO P2/H1 mice. We found that a vast majority of cKO P2/H1 mice contained activated microglia cells and patches of apoptotic neurons, the latter especially evident in recently-deceased mice. A gene-expression profile of individual brains showed clear induction of different pro-inflammatory cytokines (e.g. *TNFα* and *IL-1β*) in cKO P2/H1 mice compared to cKO P2 mice. These cytokines are known as main contributors in several neurodegenerative disorders and are typically produced by glia cells, including microglia and astrocytes, as well as neurons.[40-43] Additionally, the vascular growth factor *VEGFA*,[44] the chemokine receptor *CXCR4,*[45-47] and the multifunctional growth factor *TGFβ1*,[48,49] were over-expressed in cKO P2/H1 brains, and are related to the initiation and/or secondary phase of neurodegeneration.

Interestingly, many of these genes, including *EPO*, have been described as HIF-2α-related genes,[25,37] suggesting that loss of HIF-1α enhances HIF-2α activity, causing brain damage as well as lethality of these mice. This idea is further supported by the observation that the HIF-1α -inducible gene, *PHD3,* and known to be an excellent negative regulator of HIF-2α,[36] is down-regulated in the brain of cKO P2/H1 compared to cKO P2 mice. In addition, cKO P2/P3 mice also display severe erythrocytosis, die prematurely and show a similar induction of the array of genes induced in the brain of cKO P2/H1. This strongly suggests that *PHD3* is an essential gene downstream of HIF-1α that protects cKO P2 mice and is not just just fine-tuning the HIF response.[50] Taken together, this strongly suggests that HIF-1α in a subset of cells in the brain, including microglia, neurons and astrocytes, protects cKO P2 mice through the induction of *PHD3* and subsequent control of the HIF-2α-activity. Other evidence for a prominent role of HIF-2α in the PHD2/HIF-1α-deficient background was supported by the two-fold increase of EPO in circulation in these mice compared to cKO P2 mice. Surprisingly, cKO P2/H1 mice did not show any significant change in hematocrit compared to cKO P2, again implying that the high RBC concentration alone was probably not the cause of their early death.

In conclusion, we have shown through several loss-of-function mutations that conditional PHD2 deficiency in kidney and brain results in an excessive HIF-2α-driven overproduction of EPO. However, HIF-1α serves as a protective factor in these mice, providing new insights to a potential interplay with HIF-2α and PHD3 (Figure 6D). Additionally, these findings have implications for pharmacological strategies that aim at inducing erythropoiesis. Whereas specific inhibition of PHD2 might be beneficial, compounds that simultaneously target all PHDs can ultimately be harmful.

Acknowledgments

K.F, J.K, R.P.S., S.M. and A.M. were supported by the Emmy Noether program (the Deutsche Forschungsgemeinschaft - DFG, Germany). B.W. is an Emmy Noether fellow. This work was supported by grants from the MeDDrive-Programm (TU Dresden, Germany) to B.W., the DFG (WI 3291/1-1 and 1-2 to B.W. and FA225/22 to J.F.) and the Swiss National Science Foundation to M.G. This work was also partially supported by NIH grant 5R01EY019721 to G-H.F. The authors also like to thank the teams of Dr. Roland Jung and Beate Gnauk for excellent technical support. The work was performed as collaborative project within the COST Action TD0901 "HypoxiaNet".

Author contribution

F.K., J.K, R.P.S, S.M. and A.M designed and performed the experiments, analyzed the data and helped write the manuscript. A.W. provided tools and helpful discussions. V.I. performed experiments and helped write the manuscript. S.J, K.W. and K.G. did pathological analysis and provided helpful discussions. M.M., A.M.S. D.P., T.R provided helpful discussions and analyzed data. T.O. performed important experiments. S.B. supervised the hematological analysis. G.Br., G.F., D.R.G. and S.B, provided helpful tools. G.Ba. supervised all pathological experiments and provided helpful discussions. T.C., J.F and M.G. provided tools, helpful discussions and helped write the manuscript. B.W., designed the study, supervised the overall project, performed experiments, analyzed the data and wrote the manuscript.

Conflict of interest

The authors declare that there are no competing financial interests.

References

1. Lee FS, Percy MJ. The HIF pathway and erythrocytosis. *Annu Rev Pathol*. 2010;6:165-192.

2. Fandrey J. Oxygen-dependent and tissue-specific regulation of erythropoietin gene expression. *Am J Physiol Regul Integr Comp Physiol*. 2004;286(6):R977-988.

3. Weidemann A, Johnson RS. Nonrenal regulation of EPO synthesis. *Kidney Int*. 2009;75(7):682-688.

4. Ebert BL, Bunn HF. Regulation of the erythropoietin gene. *Blood*. 1999;94(6):1864-1877.

5. Semenza GL, Wang GL. A nuclear factor induced by hypoxia via de novo protein synthesis binds to the human erythropoietin gene enhancer at a site required for transcriptional activation. *Mol Cell Biol*. 1992;12(12):5447-5454.

6. Stroka DM, Burkhardt T, Desbaillets I, et al. HIF-1 is expressed in normoxic tissue and displays an organ-specific regulation under systemic hypoxia. *Faseb J*. 2001;15(13):2445-2453.

7. Rankin EB, Biju MP, Liu Q, et al. Hypoxia-inducible factor-2 (HIF-2) regulates hepatic erythropoietin in vivo. *J Clin Invest*. 2007;117(4):1068-1077.

8. Wiesener MS, Jurgensen JS, Rosenberger C, et al. Widespread hypoxia-inducible expression of HIF-2alpha in distinct cell populations of different organs. *Faseb J*. 2003;17(2):271-273.

9. Fandrey J, Gorr TA, Gassmann M. Regulating cellular oxygen sensing by hydroxylation. *Cardiovasc Res*. 2006;71(4):642-651.

10. Scortegagna M, Ding K, Zhang Q, et al. HIF-2alpha regulates murine hematopoietic development in an erythropoietin-dependent manner. *Blood*. 2005;105(8):3133-3140.

11. Takubo K, Goda N, Yamada W, et al. Regulation of the HIF-1alpha level is essential for hematopoietic stem cells. *Cell Stem Cell*. 2010;7(3):391-402.

12. Berra E, Benizri E, Ginouves A, Volmat V, Roux D, Pouyssegur J. HIF prolyl-hydroxylase 2 is the key oxygen sensor setting low steady-state levels of HIF-1alpha in normoxia. *Embo J*. 2003;22(16):4082-4090.

13. Takeda K, Ho VC, Takeda H, Duan LJ, Nagy A, Fong GH. Placental but not heart defects are associated with elevated hypoxia-inducible factor alpha levels in mice lacking prolyl hydroxylase domain protein 2. *Mol Cell Biol*. 2006;26(22):8336-8346.

14. Mazzone M, Dettori D, Leite de Oliveira R, et al. Heterozygous deficiency of PHD2 restores tumor oxygenation and inhibits metastasis via endothelial normalization. *Cell*. 2009;136(5):839-851.

15. Percy MJ, Zhao Q, Flores A, et al. A family with erythrocytosis establishes a role for prolyl hydroxylase domain protein 2 in oxygen homeostasis. *Proc Natl Acad Sci U S A*. 2006;103(3):654-659.

16. Ladroue C, Carcenac R, Leporrier M, et al. PHD2 mutation and congenital erythrocytosis with paraganglioma. *N Engl J Med*. 2008;359(25):2685-2692.

17. Al-Sheikh M, Moradkhani K, Lopez M, Wajcman H, Prehu C. Disturbance in the HIF-1alpha pathway associated with erythrocytosis: further evidences brought by frameshift and nonsense mutations in the prolyl hydroxylase domain protein 2 (PHD2) gene. *Blood Cells Mol Dis*. 2008;40(2):160-165.

18. Percy MJ, Furlow PW, Beer PA, Lappin TR, McMullin MF, Lee FS. A novel erythrocytosis-associated PHD2 mutation suggests the location of a HIF binding groove. *Blood*. 2007;110(6):2193-2196.

19. Gordeuk VR, Sergueeva AI, Miasnikova GY, et al. Congenital disorder of oxygen sensing: association of the homozygous Chuvash polycythemia VHL mutation with thrombosis and vascular abnormalities but not tumors. *Blood*. 2004;103(10):3924-3932.

20. Semenza GL. Involvement of oxygen-sensing pathways in physiologic and pathologic erythropoiesis. *Blood*. 2009;114(10):2015-2019.

21. Takeda K, Aguila HL, Parikh NS, et al. Regulation of adult erythropoiesis by prolyl hydroxylase domain proteins. *Blood*. 2008;111(6):3229-3235.

22. Minamishima YA, Moslehi J, Bardeesy N, Cullen D, Bronson RT, Kaelin WG, Jr. Somatic inactivation of the PHD2 prolyl hydroxylase causes polycythemia and congestive heart failure. *Blood*. 2008;111(6):3236-3244.

23. Gough PJ, Gordon S, Greaves DR. The use of human CD68 transcriptional regulatory sequences to direct high-level expression of class A scavenger receptor in macrophages in vitro and in vivo. *Immunology*. 2001;103(3):351-361.

24. Shimshek DR, Kim J, Hubner MR, et al. Codon-improved Cre recombinase (iCre) expression in the mouse. *Genesis*. 2002;32(1):19-26.

25. Gruber M, Hu CJ, Johnson RS, Brown EJ, Keith B, Simon MC. Acute postnatal ablation of Hif-2alpha results in anemia. *Proc Natl Acad Sci U S A*. 2007;104(7):2301-2306.

26. Frede S, Freitag P, Geuting L, Konietzny R, Fandrey J. Oxygen-regulated expression of the erythropoietin gene in the human renal cell line REPC. *Blood*. 2011;117(18):4905-4914.

27. Ruschitzka FT, Wenger RH, Stallmach T, et al. Nitric oxide prevents cardiovascular disease and determines survival in polyglobulic mice overexpressing erythropoietin. *Proc Natl Acad Sci U S A*. 2000;97(21):11609-11613.

28. Kapitsinou PP, Liu Q, Unger TL, et al. Hepatic HIF-2 regulates erythropoietic responses to hypoxia in renal anemia. *Blood*. 2010;116(16):3039-3048.

29. Percy MJ, Furlow PW, Lucas GS, et al. A gain-of-function mutation in the HIF2A gene in familial erythrocytosis. *N Engl J Med*. 2008;358(2):162-168.

30. Percy MJ, Beer PA, Campbell G, et al. Novel exon 12 mutations in the HIF2A gene associated with erythrocytosis. *Blood*. 2008;111(11):5400-5402.

31. Pan X, Suzuki N, Hirano I, Yamazaki S, Minegishi N, Yamamoto M. Isolation and characterization of renal erythropoietin-producing cells from genetically produced anemia mice. *PLoS One*. 2011;6(10):e25839.

32. Bernaudin M, Bellail A, Marti HH, et al. Neurons and astrocytes express EPO mRNA: oxygen-sensing mechanisms that involve the redox-state of the brain. *Glia*. 2000;30(3):271-278.

33. Socolovsky M. Molecular insights into stress erythropoiesis. *Curr Opin Hematol*. 2007;14(3):215-224.

34. Weidemann A, Kerdiles YM, Knaup KX, et al. The glial cell response is an essential component of hypoxia-induced erythropoiesis in mice. *J Clin Invest*. 2009;119(11):3373-3383.

35. Wagner KF, Katschinski DM, Hasegawa J, et al. Chronic inborn erythrocytosis leads to cardiac dysfunction and premature death in mice overexpressing erythropoietin. *Blood*. 2001;97(2):536-542.

36. Appelhoff RJ, Tian YM, Raval RR, et al. Differential function of the prolyl hydroxylases PHD1, PHD2, and PHD3 in the regulation of hypoxia-inducible factor. *J Biol Chem*. 2004;279(37):38458-38465.

37. Imtiyaz HZ, Williams EP, Hickey MM, et al. Hypoxia-inducible factor 2alpha regulates macrophage function in mouse models of acute and tumor inflammation. *J Clin Invest*. 2010;120(8):2699-2714.

38. Jefferson JA, Escudero E, Hurtado ME, et al. Excessive erythrocytosis, chronic mountain sickness, and serum cobalt levels. *Lancet*. 2002;359(9304):407-408.

39. Klotzsche-von Ameln A, Muschter A, Mamlouk S, et al. Inhibition of HIF Prolyl Hydroxylase-2 Blocks Tumor Growth in Mice through the Antiproliferative Activity of TGFbeta. *Cancer Res*. 2011;71(9):3306-3316.

40. Li C, Zhao R, Gao K, et al. Astrocytes: implications for neuroinflammatory pathogenesis of Alzheimer's disease. *Curr Alzheimer Res*. 2011;8(1):67-80.

41. Lu Y, Zhu L, Gao YJ. Pain-related aversion induces astrocytic reaction and proinflammatory cytokine expression in the anterior cingulate cortex in rats. *Brain Res Bull*. 2011;84(2):178-182.

42. Smith JA, Das A, Ray SK, Banik NL. Role of pro-inflammatory cytokines released from microglia in neurodegenerative diseases. *Brain Res Bull*. 2012;87(1):10-20.

43. Kumar M, Verma S, Nerurkar VR. Pro-inflammatory cytokines derived from West Nile virus (WNV)-infected SK-N-SH cells mediate neuroinflammatory markers and neuronal death. *J Neuroinflammation*. 2010;7:73.

44. Storkebaum E, Carmeliet P. VEGF: a critical player in neurodegeneration. *J Clin Invest*. 2004;113(1):14-18.

45. Miller JT, Bartley JH, Wimborne HJ, et al. The neuroblast and angioblast chemotaxic factor SDF-1 (CXCL12) expression is briefly up regulated by reactive astrocytes in brain following neonatal hypoxic-ischemic injury. *BMC Neurosci*. 2005;6:63.

46. Khan MZ, Shimizu S, Patel JP, et al. Regulation of neuronal P53 activity by CXCR 4. *Mol Cell Neurosci*. 2005;30(1):58-66.

47. Shimoji M, Pagan F, Healton EB, Mocchetti I. CXCR4 and CXCL12 expression is increased in the nigro-striatal system of Parkinson's disease. *Neurotox Res*. 2009;16(3):318-328.

48. Swardfager W, Lanctot K, Rothenburg L, Wong A, Cappell J, Herrmann N. A meta-analysis of cytokines in Alzheimer's disease. *Biol Psychiatry*. 2010;68(10):930-941.

49. Town T, Laouar Y, Pittenger C, et al. Blocking TGF-beta-Smad2/3 innate immune signaling mitigates Alzheimer-like pathology. *Nat Med*. 2008;14(6):681-687.

50. Minamishima YA, Moslehi J, Padera RF, Bronson RT, Liao R, Kaelin WG, Jr. A feedback loop involving the Phd3 prolyl hydroxylase tunes the mammalian hypoxic response in vivo. *Mol Cell Biol*. 2009;29(21):5729-5741.

Figure legends

Figure 1. Conditional deficient PHD2 mice display severe HIF-2α -induced erythrocytosis. (A) Compared to WT mice, cKO P2 show profound redness of the snout and paws. (B) Body weight of WT and cKO P2 mice was measured on a weekly basis until adulthood. No significant difference was observed after week 8 (n = 5-11). (C) Percentage of red blood cell volume per blood volume (hematocrit-hct) from mice was measured every two weeks until adulthood, displaying highly significant differences from week 4 after birth (n = 5-10). (D) Hcts in cKO P2/H1 remained as high as in cKO P2 mice whereas cKO P2/H2 mice showed even slightly but significantly lower hcts than WTs (n = 6-15). (E and F) RBC count (n = 7-32) and hemoglobin (n = 6-22) concentration in freshly isolated blood samples demonstrate that HIF-2α but not HIF-1α induces erythrocytosis due to loss of PHD2. All data are mean ± s.e.m. $*P < 0.05$, $**P < 0.01$, $***P < 0.001$.

Figure 2. Loss of PHD2 in cKO P2 mice leads to induction of EPO in kidney and brain. (A) Erythropoietin (EPO) concentration in plasma measured by ELISA in the plasma of WT, cKO P2, cKO P2/H1 and cKO P2/H2 mice (n = 6-22). cKO mice contain on average 6 times more EPO in the circulation than their WT littermates, whereas cKO P2/H1 mice have over 17 times more EPO. No difference between WT and cKO P2/H2 was found. (B) mRNA levels in total extracts from kidney and brain (n = 5-15) is markedly induced compared to WT but not significantly different between cKO P2 and cKO P2/H1 mice because of the high variation between individual samples (n = 7-11). No difference between WT and cKO P2/H2 could be shown. (C) The renal derived human cell line (REPC)[26] was tested for the expression of EPO and CD68 grown under normoxic and hypoxic conditions via RT-PCR, showing the expected

EPO induction and expression of CD68 under both conditions, suggesting a potential link between cre-expression, PHD2 inactivation and subsequent EPO expression in these cell types. (D) Astrocytes isolated from the cerebral cortex of five day old pups show a significantly reduced PHD2 content in cKO P2 versus WT mice (n = 3). (E) Typical IHC on brain sections for PHD2 (red) with or without NeuN (green) show a majority of PHD2-negative neurons in the brain of cKO P2 mice (depicted by arrow heads) but not in WT. (F) WT and cKO P2 mice were lethally irradiated and received cKO P2 or WT bone marrow (BM) respectively. Hematocrits were measured 4 months after transfer. BM from either genotype did not change hcts in the recipient (n = 6-23). Scale bar in (E) represents 50µm All data are mean ± s.e.m. N.S. is not significant and *P< 0.05, *** P < 0.001.

Figure 3. Erythrocytosis is mainly caused by extramedullary erythropoiesis in the spleen. (A and B) Representative sections of WT and cKO P2 spleens (H&E) show an extensive structural loss and an augmentation of nucleated cells in erythrocytotic cKO P2 mice. (C) Spleen weight of WT and cKO P2 mice (n = 10-16). (D-G) Representative FACS staining profiles of (D and E) megakaryocyte-erythrocyte progenitors (MEP) (n = 6) and (F and G) erythroblasts (EB) (n = 7) in BM and spleen of WT and cKO P2 showing that the overproduction of RBCs is mainly executed in the spleen. Scale bars represent 500µm. All data are mean ± s.e.m. *P < 0.05, ***P < 0.001.

Figure 4. cKO P2 mice show thrombocytopenia but no early lethality, while cKO P2/H1 die prematurely. (A) Thrombocyte concentrations in the blood of WT and cKO P2 mice until adulthood reveal a significant reduction of circulating platelets per volume of blood in cKO P2

mice (n = 5-10). WT is represented by black squares and cKO P2 by red triangles. (B) 8-10 week old mice were bled and thrombocytes measured in a fixed volume of blood showing thrombocytopenia in cKO and cKO P2/H1 mice compared to WT and cKO P2/H2 mice (n = 6-7). (C-D) WT and cKO P2 kidneys stained with acid Fuchsin orange-G show no signs of microvascular thrombosis suggesting that platelets are not trapped within blood clots. (E) Instead, the total blood volume of cKO P2 mice was significantly increased compared to WT mice (n = 9-10). (F) Nine cKO P2 mice (five females and four males) were kept for 20 months. Mice were bled every 4 months to measure hematocrits. No significant differences in hcts were found and none of the mice died before the end of the experiment. (G) cKO P2/H1 (n = 17) and cKO P2 (n = 15) mice were followed for 20 weeks. cKO P2/H1 mice began to die from week five after birth. By week sixteen, 16 out of 17 mice were deceased. No cKO P2 mice died during the course of this experiment. Scale bars represent 100 µm. All data are mean ± s.e.m. $^{**}P < 0.01$, $^{***}P < 0.001$.

Figure 5. HIF1a serves as a protective factor to prevent brain damage. (A-C) IHC on brain sections from WT, cKO P2 and cKO P2/H1 for Iba1 (brown) showing more activated microglia cells in brain sections of a cKO P2/H1 mouse. (D-F) IHC on brain sections from a freshly deceased cKO P2/H1 mouse for (D) cleaved-caspase3 (cl-Casp3) (red), (E) neurons (NeuN) (green) and (F) a merged picture combined with DAPI (white arrows depict typical examples of cl-Casp3^{+} neurons). No obvious cl-Casp3 staining was detected in WT or cKO P2 brains (data not shown). (G) Expression profile (qRT-PCR) of different genes in the lysate of the entire brain of cKO P2 and cKO P2/H1 mice in relation to their respective WT littermates (n = 5-9). All data are mean ± s.e.m. $^{*}P< 0.05$. Scale bars in (A-C) 100µm and (D-F) 50µm.

Figure 6. Mice deficient for PHD2 and PHD3 display erythrocytosis and die prematurely. (A) cKO P2/P3 mice show enhanced Hcts compared to their WT littermates (n = 5). (B) WT, PHD3$^{-/-}$ and cKO P2/P3 mice were followed for 20 weeks. cKO P2/P3 mice began to die shortly after birth (n = 7). (C) Expression profile (qRT-PCR) of different genes in the lysate of the entire brain of cKO P2 and cKO P2/P3 mice in relation to their respective WT littermates. *p<0.05 is significantly different from cKO P2 samples (expression relative to their WT littermates) (n = 5-7). (D) Schematic overview of the different genetic mouse models that were generated in this study showing non-lethal erythrocytotic cKO P2 mice that display a perfect balance between the protective HIF-1α activity and detrimental HIF-2α activity in the brain. In cKO P2/H1 mice this balance is disturbed in favor of the HIF-2α activity leading to early lethality in the mice. All data are mean ± s.e.m. *P< 0.05, **P < 0.01

Figure 1

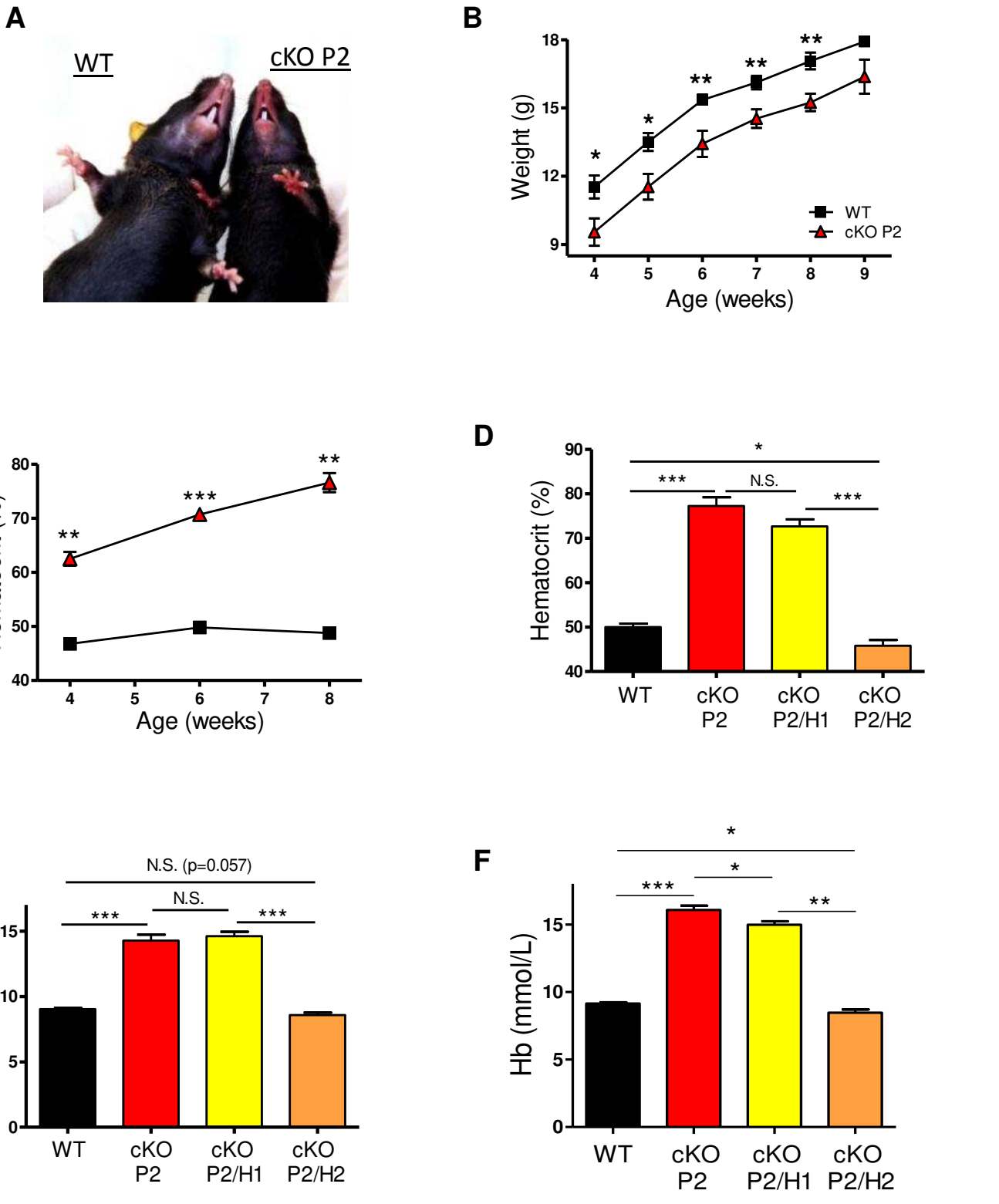
A
WT
cKO P2
B
Weight (g)
Age (weeks)
WT
cKO P2
C
Hematocrit (%)
Age (weeks)
D
Hematocrit (%)
N.S.
WT
cKO P2
cKO P2/H1
cKO P2/H2
E
RBC (x10^12/ L)
N.S. (p=0.057)
N.S.
WT
cKO P2
cKO P2/H1
cKO P2/H2
F
Hb (mmol/L)
WT
cKO P2
cKO P2/H1
cKO P2/H2

Figure 2

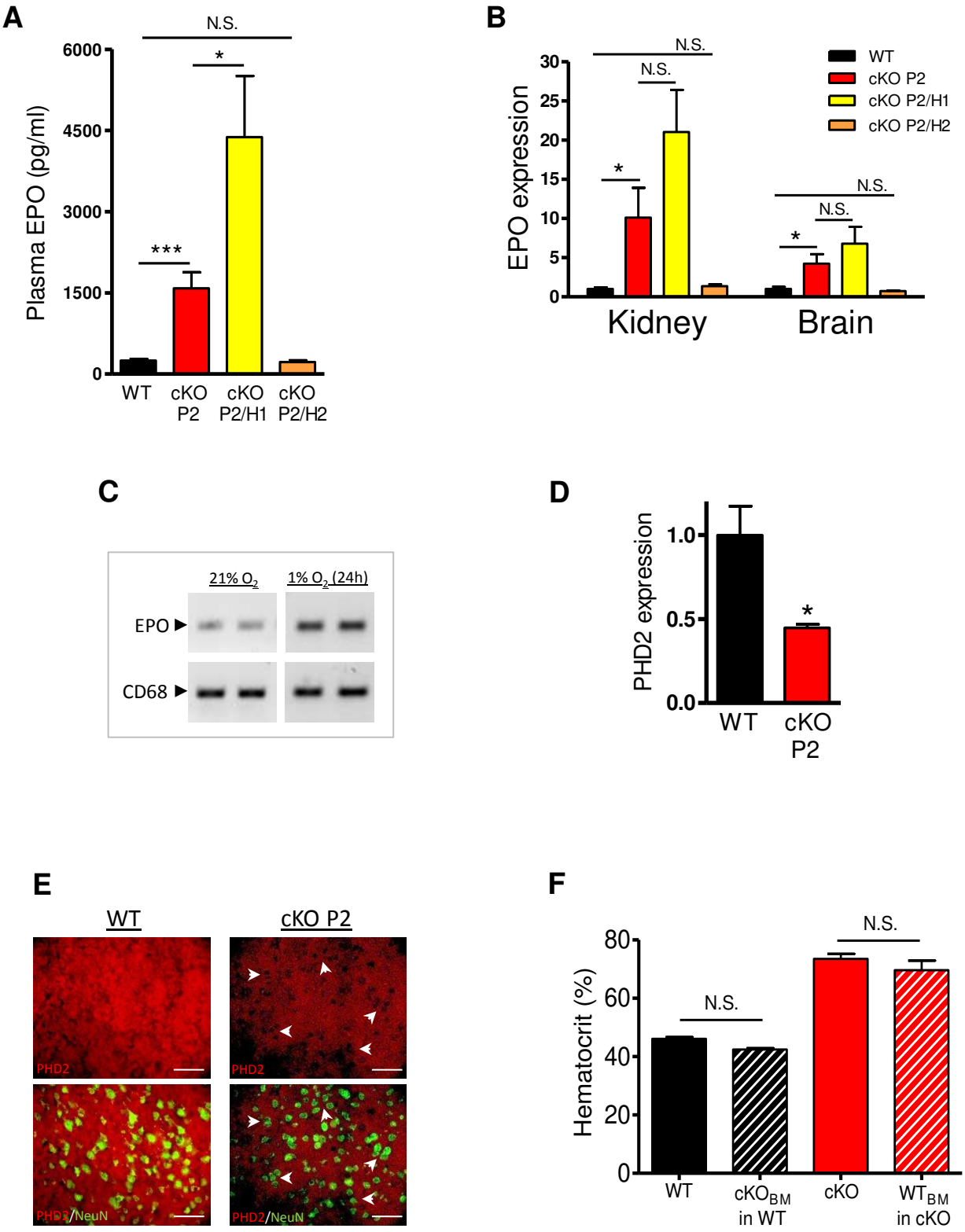
A
N.S.
*
***
Plasma EPO (pg/ml)
6000
4500
3000
1500
0
WT
cKO P2
cKO P2/H1
cKO P2/H2
B
N.S.
N.S.
*
N.S.
N.S.
*
EPO expression
30
25
20
15
10
5
0
WT
cKO P2
cKO P2/H1
cKO P2/H2
Kidney
Brain
C
21% O2
1% O2 (24h)
EPO
CD68
D
PHD2 expression
1.0
0.5
0.0
*
WT
cKO P2
E
WT
cKO P2
PHD2
PHD2
PHD2/NeuN
PHD2/NeuN
F
N.S.
N.S.
Hematocrit (%)
80
60
40
20
0
WT
cKOBM in WT
cKO
WTBM in cKO

Figure 3

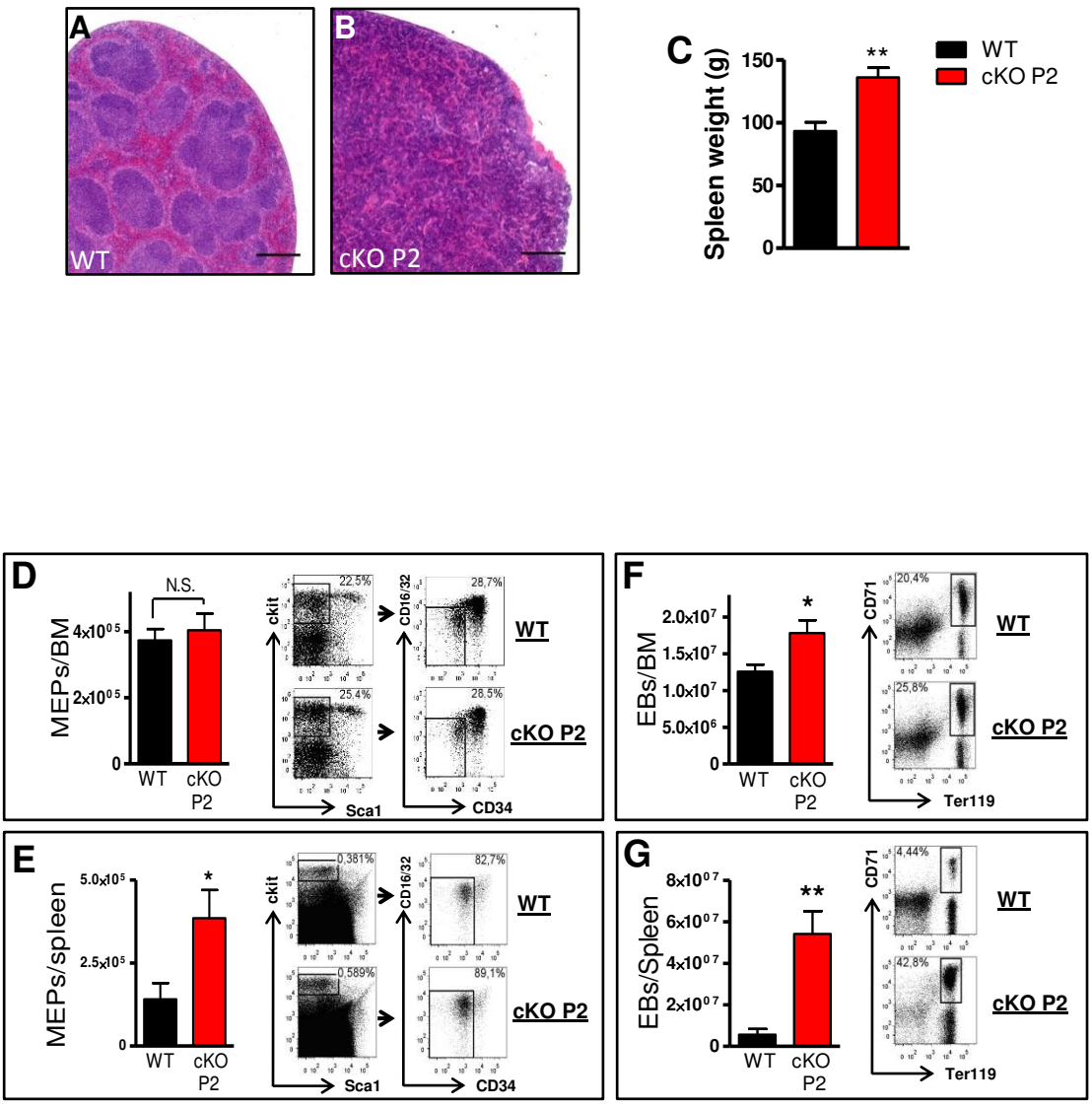
A
WT
B
cKO P2
C
Spleen weight (g)
150
100
50
0
**
WT
cKO P2
D
MEPs/BM
4x10^05
2x10^05
0
N.S.
WT
cKO P2
ckit
22.5%
25.4%
Sca1
CD16/32
28,7%
28.5%
CD34
WT
cKO P2
F
EBs/BM
2.0x10^7
1.5x10^7
1.0x10^7
5.0x10^6
0
*
WT
cKO P2
CD71
20,4%
25,8%
Ter119
WT
cKO P2
E
MEPs/spleen
5.0x10^5
2.5x10^5
0
*
WT
cKO P2
ckit
0,381%
0,589%
Sca1
CD16/32
82,7%
89,1%
CD34
WT
cKO P2
G
EBs/Spleen
8x10^07
6x10^07
4x10^07
2x10^07
0
**
WT
cKO P2
CD71
4,44%
42,8%
Ter119
WT
cKO P2

Figure 4

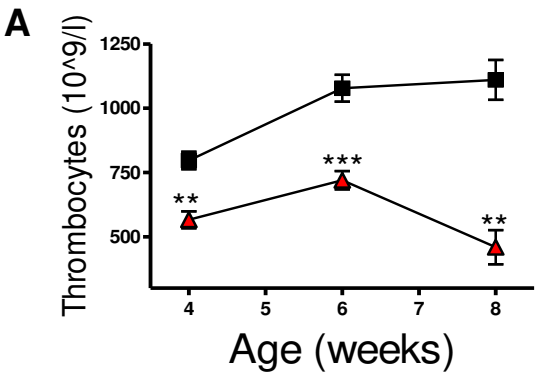
A
Thrombocytes (10^9/l)
1250
1000
750
500
**
***
**
4
5
6
7
8
Age (weeks)

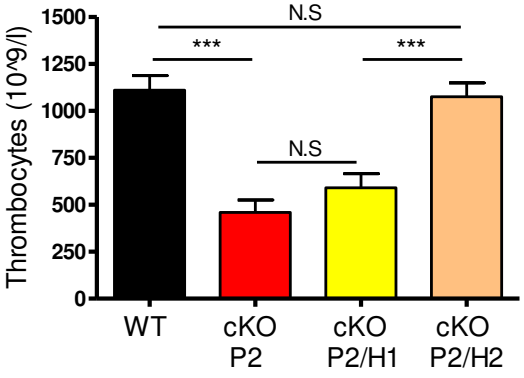
B
Thrombocytes (10^9/l)
1500
1250
1000
750
500
250
0
N.S
***
***
N.S
WT
cKO P2
cKO P2/H1
cKO P2/H2

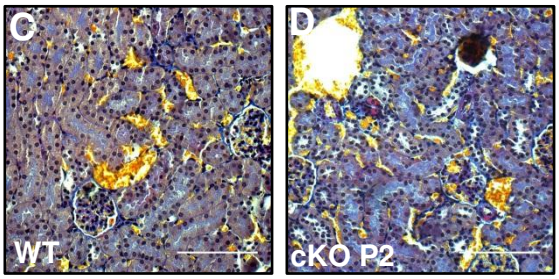
C
WT
D
cKO P2

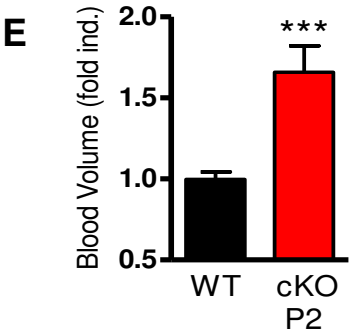
E
Blood Volume (fold ind.)
2.0
1.5
1.0
0.5
***
WT
cKO P2

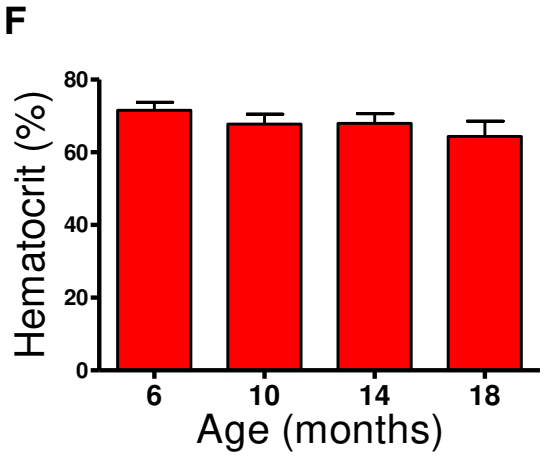
F
Hematocrit (%)
80
60
40
20
0
6
10
14
18
Age (months)

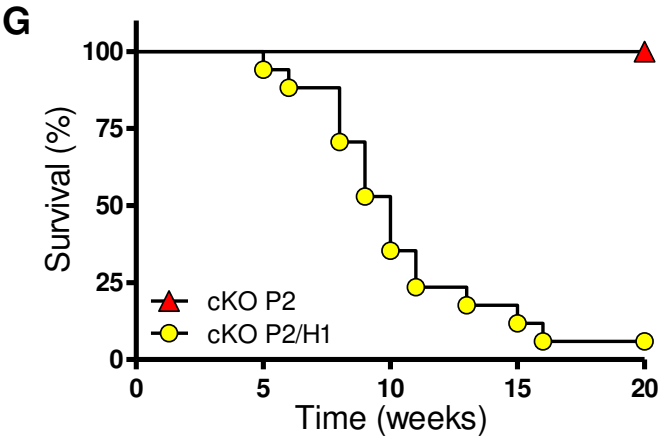
G
Survival (%)
100
75
50
25
0
cKO P2
cKO P2/H1
0
5
10
15
20
Time (weeks)

Figure 5

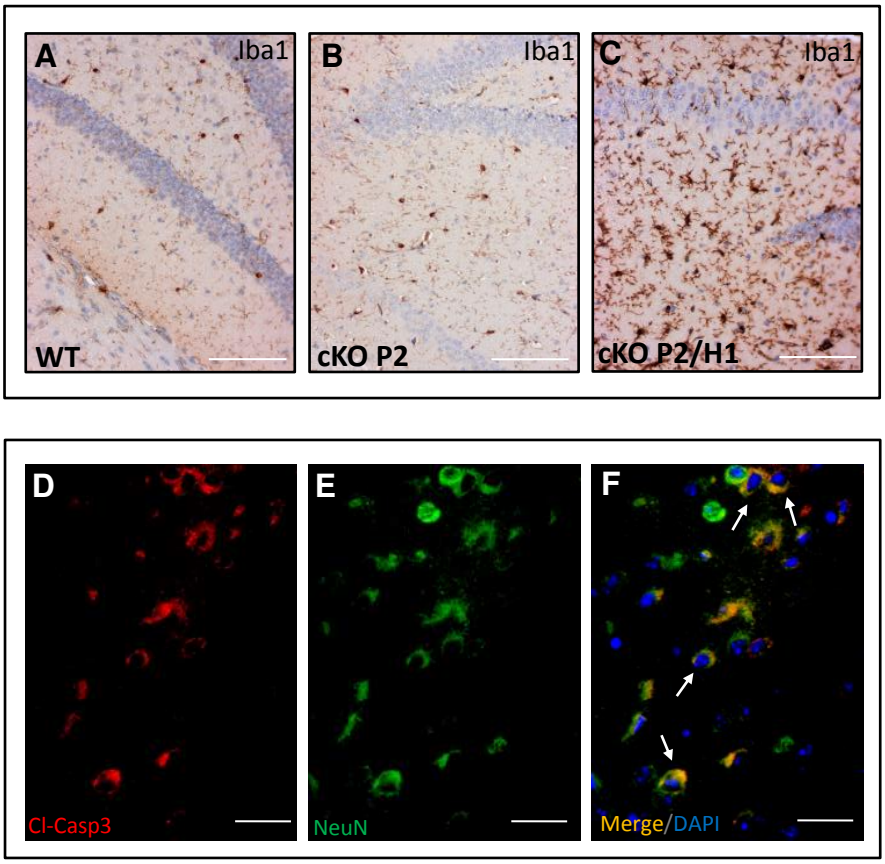
A
Iba1
WT
B
Iba1
cKO P2
C
Iba1
cKO P2/H1
D
Cl-Casp3
E
NeuN
F
Merge/DAPI

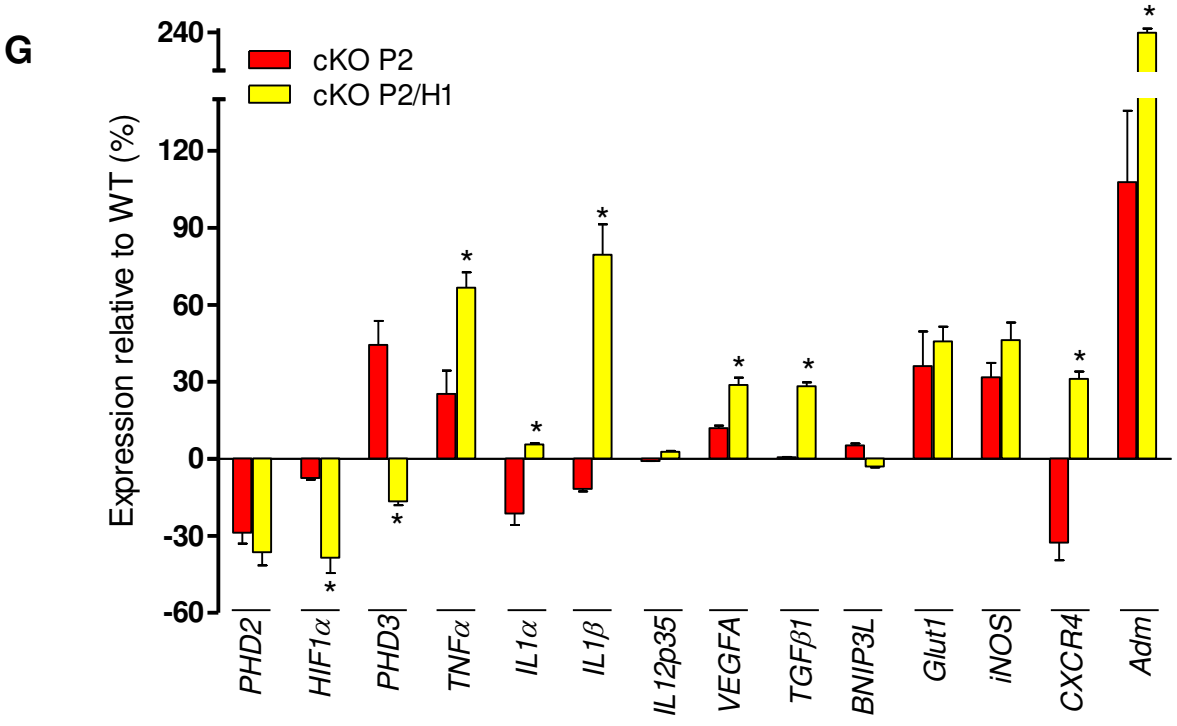
G
cKO P2
cKO P2/H1
Expression relative to WT (%)
240
120
90
60
30
0
-30
-60
PHD2
HIF1α
PHD3
TNFα
IL1α
IL1β
IL12p35
VEGFA
TGFβ1
BNIP3L
Glut1
iNOS
CXCR4
Adm

Figure 6

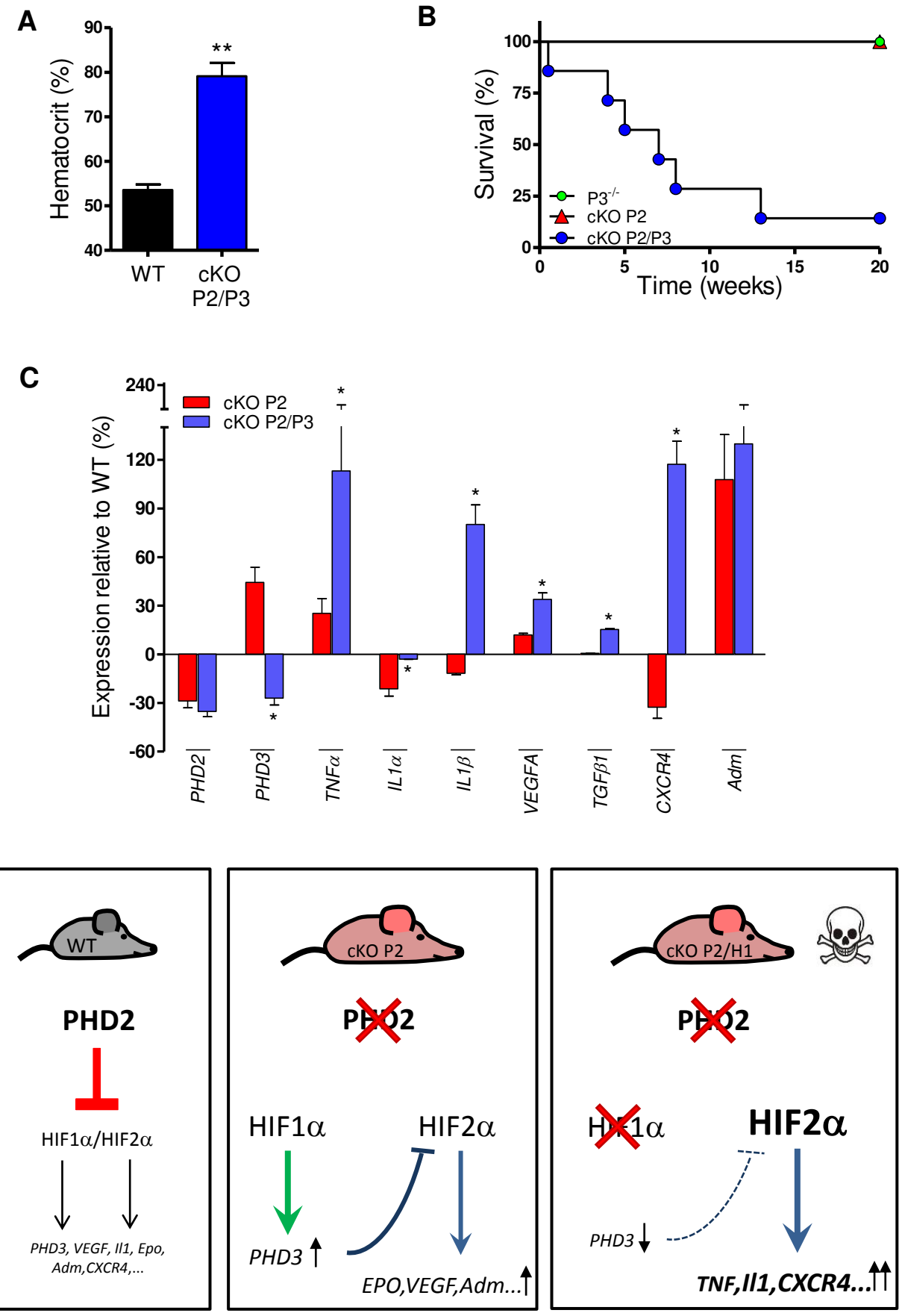
A
Hematocrit (%)
90
80
70
60
50
40
**
WT
cKO P2/P3
B
Survival (%)
100
75
50
25
0
P3-/-
cKO P2
cKO P2/P3
0
5
10
15
20
Time (weeks)
C
Expression relative to WT (%)
240
120
90
60
30
0
-30
-60
cKO P2
cKO P2/P3
PHD2
PHD3
TNFα
IL1α
IL1β
VEGFA
TGFβ1
CXCR4
Adm
D
WT
PHD2
HIF1α/HIF2α
PHD3, VEGF, Il1, Epo, Adm,CXCR4,...
cKO P2
PHD2
HIF1α
HIF2α
PHD3
EPO,VEGF,Adm...
cKO P2/H1
PHD2
HIF1α
HIF2α
PHD3
TNF,Il1,CXCR4...

Supplemental Figure 1

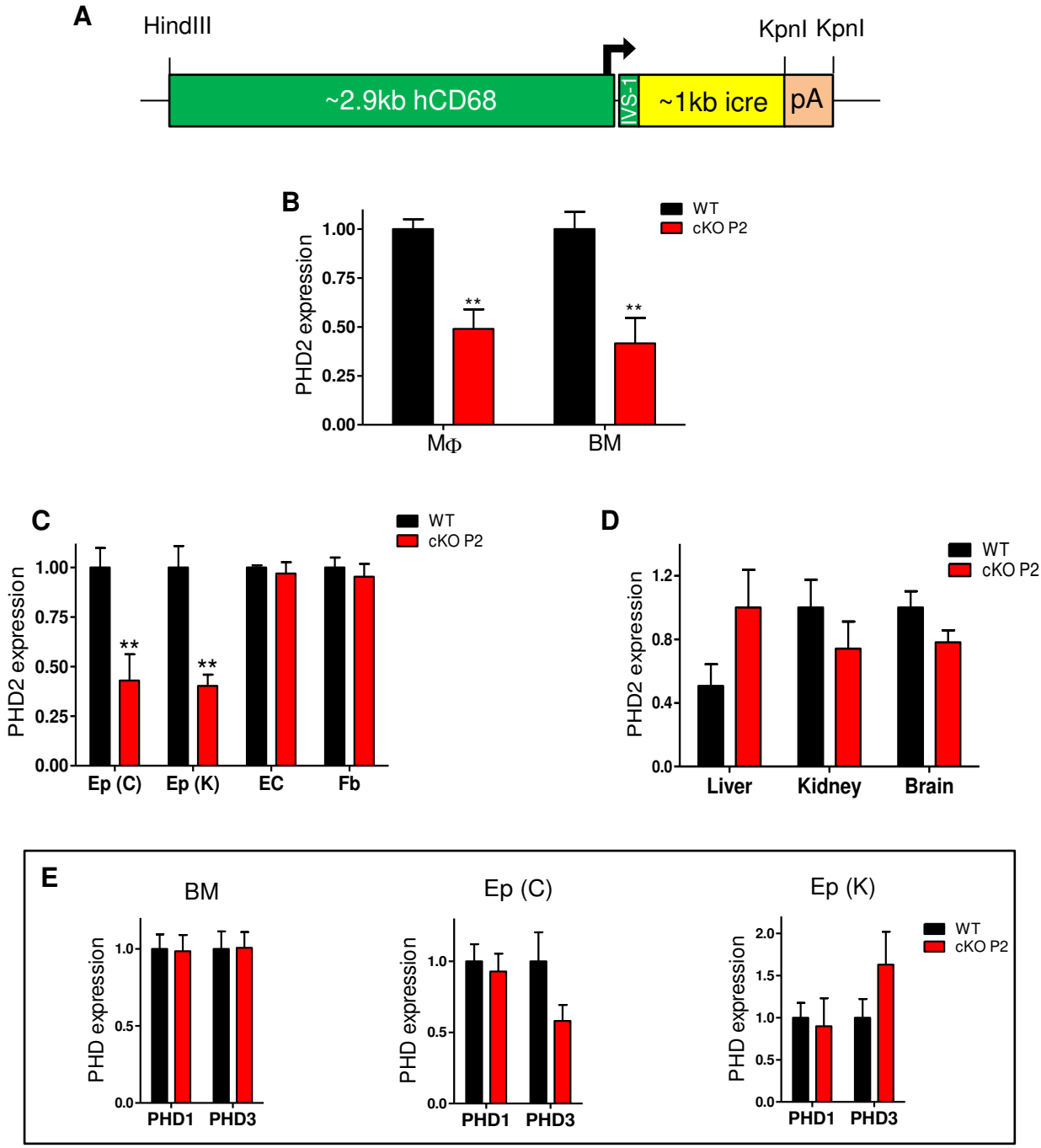

Supplemental Figure 1. Production of CD68:icre-pA and expression profile of CD68:cre-PHD2$^{f/f}$ mice. (A) Schematic representation of the pUC19-CD68-icre-pA vector constructed using classical cloning methods (icre: improved cre). All cloning steps were sequence verified and functionality of the construct tested in the RAW264 cell line. (B) Different hematopoietic cells (Macrophages (MΦ) and whole bone marrow (BM)) were isolated from WT and CD68:cre-PHD2$^{f/f}$ (cKO P2) mice and tested for the presence of PHD2 mRNA (n = 5-7). (C) Epithelial cells (colonocytes (Ep (C)) and keratinocytes (Ep (K)), lung endothelial cells (EC) and skin fibroblasts from newborns (Fb)) were isolated, (D) as well as lysates from different organs and tested for PHD2 mRNA content via qPCR (n = 5-7). (E) PHD1 and 3 expression levels in bone marrow (BM) and isolated epithelial cells out of colon and skin from WT and cKO mice (n = 3-6). No significant difference between both genotypes could be detected. All data are mean ± s.e.m. $^{**}P < 0.01$

Supplemental Figure 2

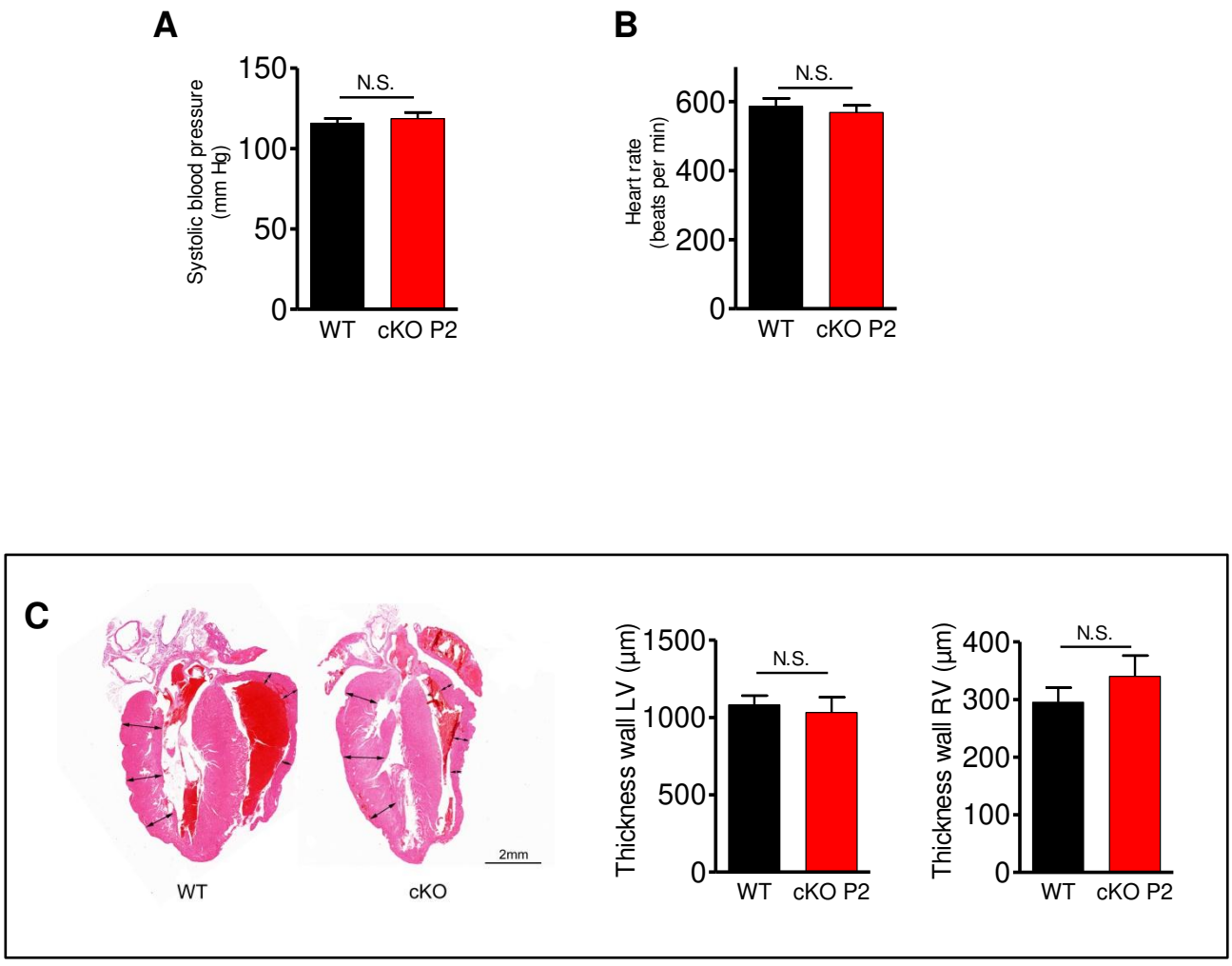

Supplemental Figure 2. Blood pressure and heart beat/hypertrophy in cKO P2 is not altered. (**A-B**) Blood pressure and heart beat of all mice were measure at the age of 8-12 weeks via the non-invasive cuff-tail method. (n = 7-9) (**C**) Sections of the heart of both phenotypes were stained with H&E and thickness of the wall of both ventricles were compared. No significant difference between WT and cKO P2 mice was detected (n = 6-8). All data are mean ± s.e.m. N.S. is not significant.

Supplemental Figure 3

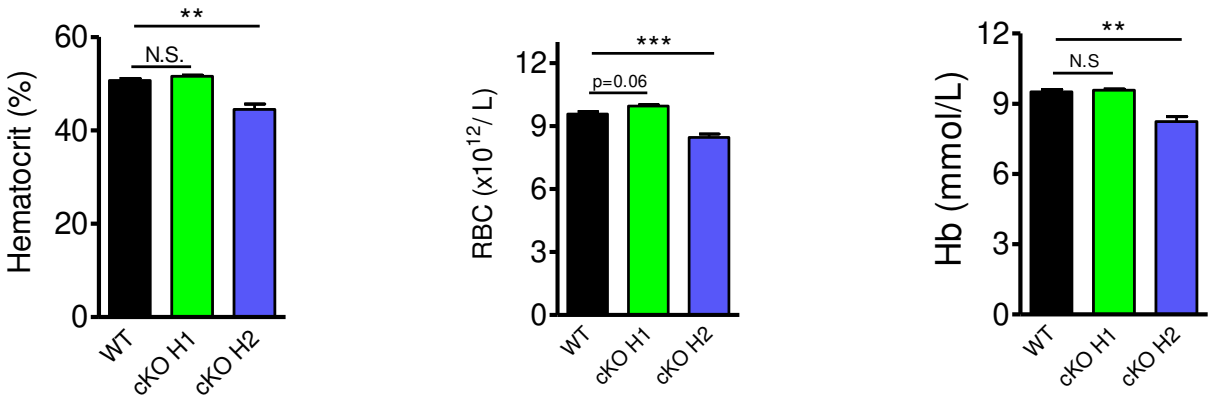

Supplemental Figure 3. Loss of HIF-2α leads to mild anemia. (**A-C**) All mice were bled at the age of 8 weeks. cKO H2 mice showed significantly lower hcts, RBC counts and hemoglobin than WTs or cKO H1 mice. This signifies the specific cre-activation in EPO producing cells driven by the hCD68 promotor and the role of HIF-2α in erythropoiesis (n = 6-9). All data are mean ± s.e.m. N.S. is not significant and *** $P < 0.001$.

Supplemental Figure 4

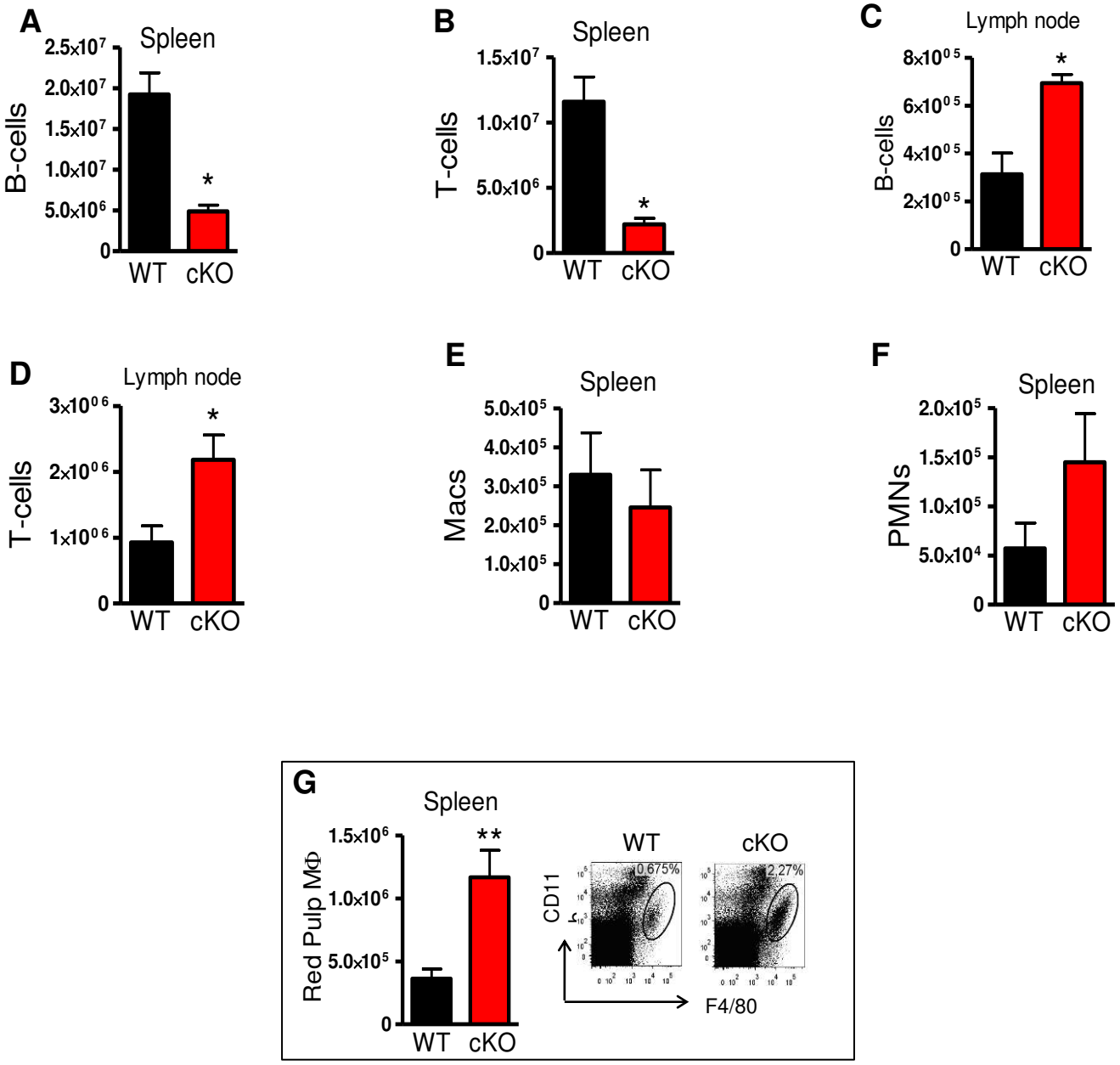

Supplemental Figure 4. cKO spleen is almost devoid of lymphocytes but not of myeloid cells. (**A** and **B**) B- and T-lymphocytes in spleen extracts from WT and cKO mice showing significant reduction in erythrocytotic mice (n = 4). (**C** and **D**) Conversely, lymph nodes (2 popliteal and 2 inguinal) from cKO mice contain more B and T lymphocytes (n = 5). (**E** and **F**) No difference was detected in myeloid cells (macrophages and PMNs) in spleen (n = 5). (**G**) However, red pulp macrophages, a subtype responsible for the elimination of RBCs, is significantly induced in cKO mice in the spleen (n = 5). All data are mean ± s.e.m. $*P < 0.05$, $**P < 0.01$.

Supplemental Figure 5

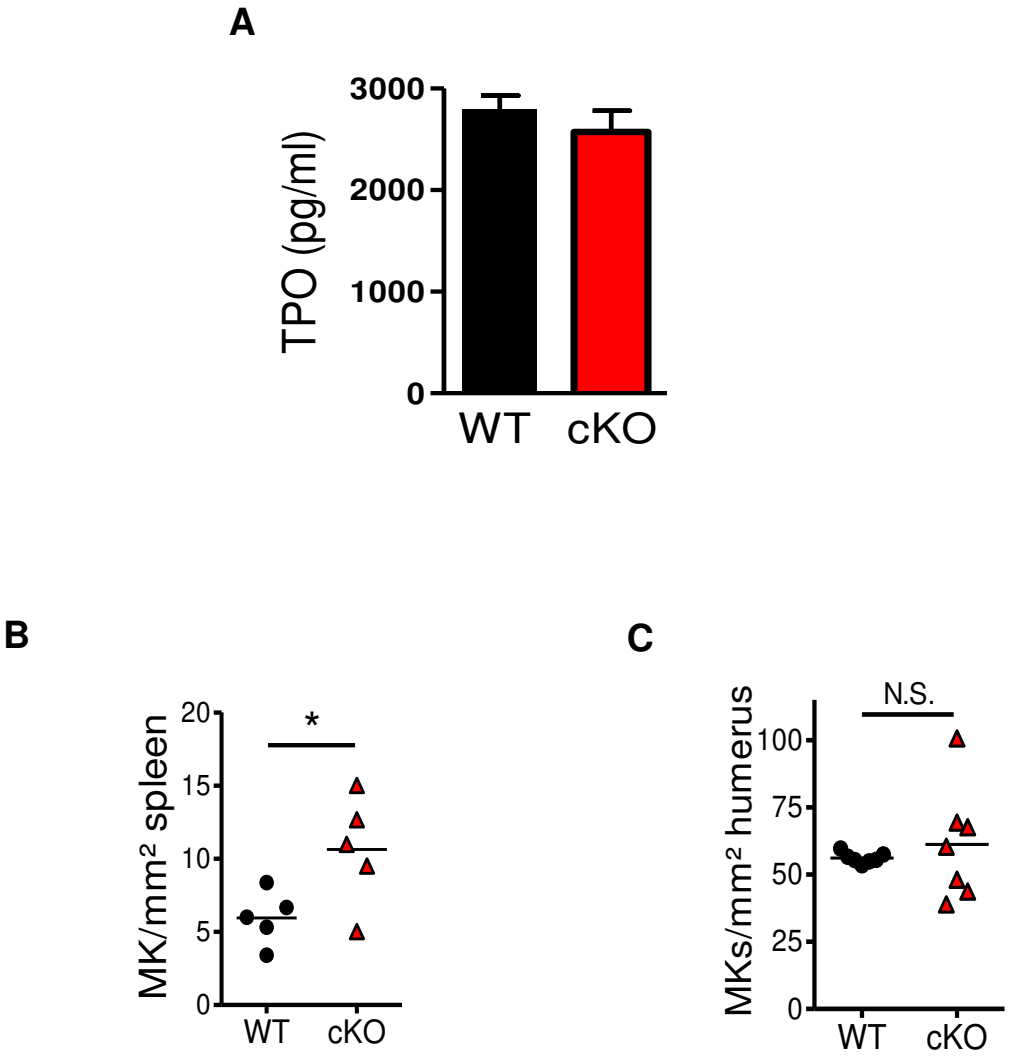

Supplemental Figure 5. cKO mice show thrombocytopenia but no reduction in its progenitors (A) Serum thrombopoietin (TPO) levels were measured via ELISA but show no difference between both genotypes (n = 7-14). (**B and C**) Megakaryocyte (MK) counting in H&E sections. cKO mice show no drop but rather an increase in total MKs per area. All data are mean ± s.e.m. N.S. is not significant and $*P < 0.05$.

Supplemental Figure 6

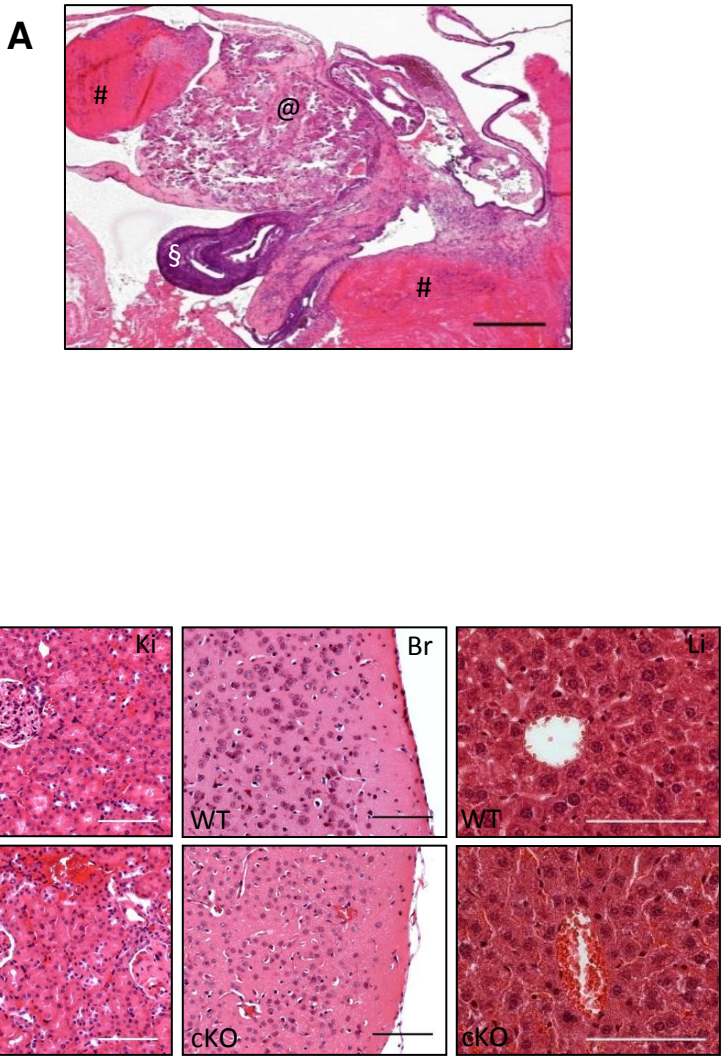

Supplemental Figure 6. cKO mice are viable without obvious pathological defects. (**A**) A regressing cyst in a 20-month old female cKO mouse localized to an ovary (§) containing fibrin deposits (#) and a large calcificated area (@). (**B**) At 20 months of age these mice were sacrificed and different organs (Ki: kidney, Br.: brain, Li: Liver) from WT and cKO mice were isolated and stained with H&E. No obvious pathological defects could be observed. Scale bar in (A) represents 500 µm and (B) 50µm.

Supplemental Figure 7

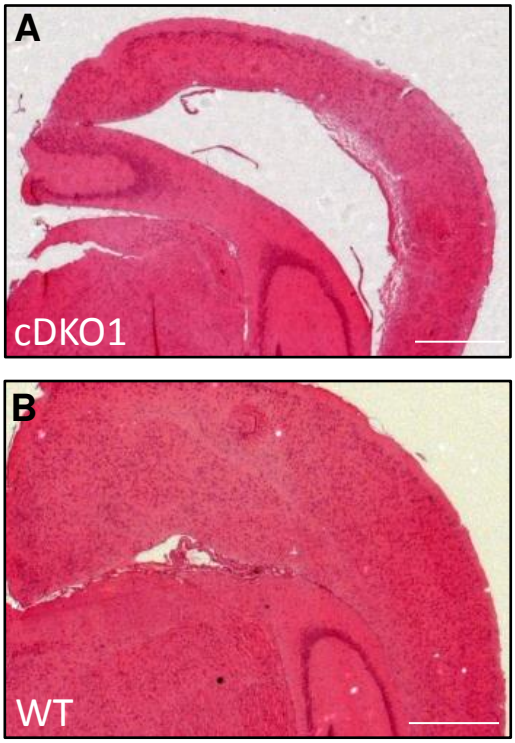

Supplemental Figure 7. Some cDKO1 mice display deformity of the head. A section of the brain of a (**A**) cDKO1 mouse with a dome-shaped skull (representative) versus a (**B**) WT littermate (H&E) showing the expanded ventricle indicating hydrocephalus. Scale bars represent 500 µm.

Supplementary Tables

TABLE 1. LIST OF PRIMERS USED TO GENOTYPE MICE

hCD68 promoter	5'-CAACTGGTGCAGACAGCCTA-3'
cre recombinase	5'-CTGCACACAGACAGGAGCAT-3'
PHD2, exon2	5'-CGCATCTTCCATCTCCATTT-3'
PHD2, intron3	5'-GGCAGTGATAACAGGTGCAA-3'
PHD2, intron1	5'-CTCACTGACCTACGCCGTGT-3'
HIF1α, intron2	5'-GCAGTTAAGAGCACTAGTTG-3'
HIF1α, intron2	5'-GGAGCTATCTCTCTAGACC-3'
HIF2α, intron2	5'-CAGGCAGTATGCCTGGCTAATTCCAGTT-3'
HIF2α, intron2	5'-CTTCTTCCATCATCTGGGATCTGGGACT-3'
HIF2α, intron1	5'-GCTAACACT GTACTGTCTGAAAGAGTAGC-3'
PHD3 fwd	5'-ATGGCCGCTGTATCACCTGTA T-3'
PHD3 Rev	5'-CCACGTTAACTCTAGAGCCACTGA-3'

TABLE 2. LIST OF PRIMERS USED FOR qRT-PCR

PHD2, exon 3	5'-AAGCCCAGTTTGCTGACATT-3'
PHD2, exon 4	5'-CTCGCTCATCTGCATCAAAA-3'
HIF1α, exon 1	5'-GGCGAGAACGAGAAGAAAAA-3'
HIF1α, exon 2	5'-AAGTGGCAACTGATGAGCAA-3'
HIF2α, exon 1	5'-GGTTAAGGAACCCAGGTGCT-3'
HIF2α, exon 2	5'-GGAAGGAGAAATCCCGTGAT-3'
EPO, exon 4	5'-CACCAGAGACCCTTCAGCTT-3'
EPO, exon 5	5'-GTGGTATCTGGAGGCGACAT-3'
PHD3, exon 2	5'-GGCCGCTGTATCACCTGTAT-3'
PHD3, exon 4	5'-TTCTGCCCTTTCTTCAGCAT-3'
TNF-α, exon3	5'-CATCTTCTCAAAATTCGAGTGACAA-3′
TNF-α, exon4	5'-TGGGAGTAGACAAGGTACAACCC-3′
hCD68 ex1 fw (h=human)	5'-GCTACTGGCAGCCCCAGGG-3′
hCD68 ex2 rev	5'-GCTCTTGGTAGTCCTGTGG-3′
Glut1 (m-slc2a) fw	5'-GTCGGGGGCATGATTGGTTCCTT-3′
Glut1 (m-slc2a) rev	5'-CTCTTGGCCCGGTTCTCCTCGTTA-3′
IL1a denes fw	5'-CCATAACCCATGATCTGGAAGAG-3′
IL1a denes rev	5'-GCTTCATCAGTTTGTATCTCAAATCAC-3′
IL1b depot fw	5'-TGTGAAATGCCACCTTTTGA-3′
IL1b depot rev	5'-GGTCAAAGGTTTGGAAGCAG-3′
Nos2 fwd	5'-GTTCTCAGCCCAACAATACAAGA-3′
Nos2 rev	5'-GTGGACGGGTCGATGTCAC-3′
TGFb1f Q	5'-CAACCCAGGTCCTTCCTAAA-3′
TGFb1r Q	5'-GGAGAGCCCTGGATACCAAC-3′
Bnip3l fw	5'-CCAAGGCCAGCACATGAGAA-3′
Bnip3l rev	5'-GCTCTCAGTCAGAAGAAG-3′
VEGFA fw	5'- GGA GAG CAG AAG TCC CAT GA -3′
VEGFA rev	5'- ACA CAG GAC GGC TTG AAG AT -3′
IL12 p35 Fwd	5'-CTAGACAAGGGCATGCTGGT-3'
IL12 p35 Rev	5'-GCTTCTCCCACAGGAGGTTT-3'
CXCR 4 Gooss Fw	5'-GAAGTGGGTTCTGGAGACTAT-3'
CXCR 4 Gooss Rev	5'-TTGCCGACTATGCCAGTCAAG-3'
Adm depot fw	5'-TGGACTTTGGGGTTTTGCTA-3'
Adm depot rev	5'-AACCAGCTTCATTCTGTGGC -3'

TABLE 3. LIST OF PRIMERS OF HOUSEHOLD GENES USED FOR NORMALISATION WITH THE qRT-PCR ΔΔCt METHOD

EF2, exon7/8	5'-AGGCCGCCATGGGTATTAAG-3'
EF2, exon8	5'-TTCAGACCTGTGGACACCACC-3'
β-actin, exon6	5'-GCTTCTAGGCGGACTGTTACTGA-3'
β-actin, exon6	5'-GCCATGCCAATGTTGTCTCTTAT-3'
mTBP, exon4	5'-TCTACCGTGAATCTTGGCTGTAAA-3'
mTBP, exon5	5'-TTCTCATGATGACTGCAGCAAA-3'
β2m, exon4	5'-ATGCACGCAGAAAGAAATAGCAA-3'
β2m, exon 4	5'-AGCTATCTAGGATATTTCCAATTTTTGAA-3'
ß2-microglobulin-h-s	5'-CTTTCAGCAAGGACTGGTCTTTC-3'
ß2-microglobulin-h-as	5'-TCACATGGTTCACACGGCAG-3'
hEF2var-s	5'-ATC CTC ACC GAC ATC ACC AAG-3'
hEF2var-as	5'-CTG CTC TGG ACA CTG GAT CTC-3'